Electronic Supplementary Material (ESI) for Organic & Biomolecular Chemistry

Supporting Information

Promiscuity of a Modular Polyketide Synthase Towards Natural and Non-Natural Extender Units

Irina Koryakina, John McArthur, Matthew M Draelos, and Gavin J Williams*

Department of Chemistry, North Carolina State University, Raleigh, NC, USA

*Corresponding author, e-mail: gavin_williams@ncsu.edu

Supporting Information Index

Data is presented in same order as main text.

Figure S1. High resolution LC-MS analysis of *holo*-Mod6TE reactions.

Reaction with 2a

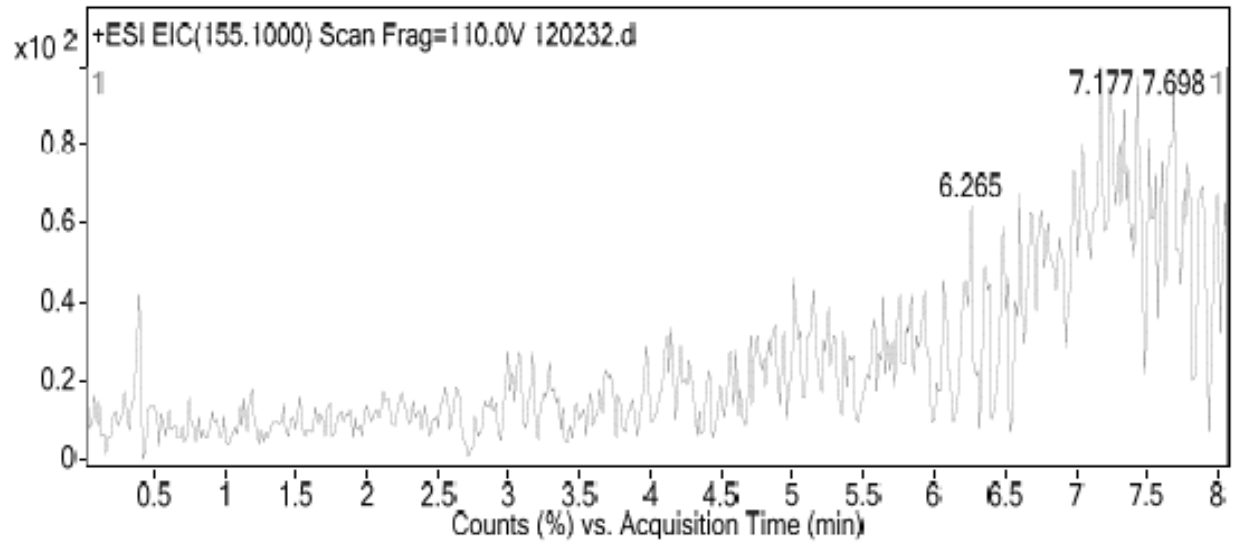

Reaction with 2b

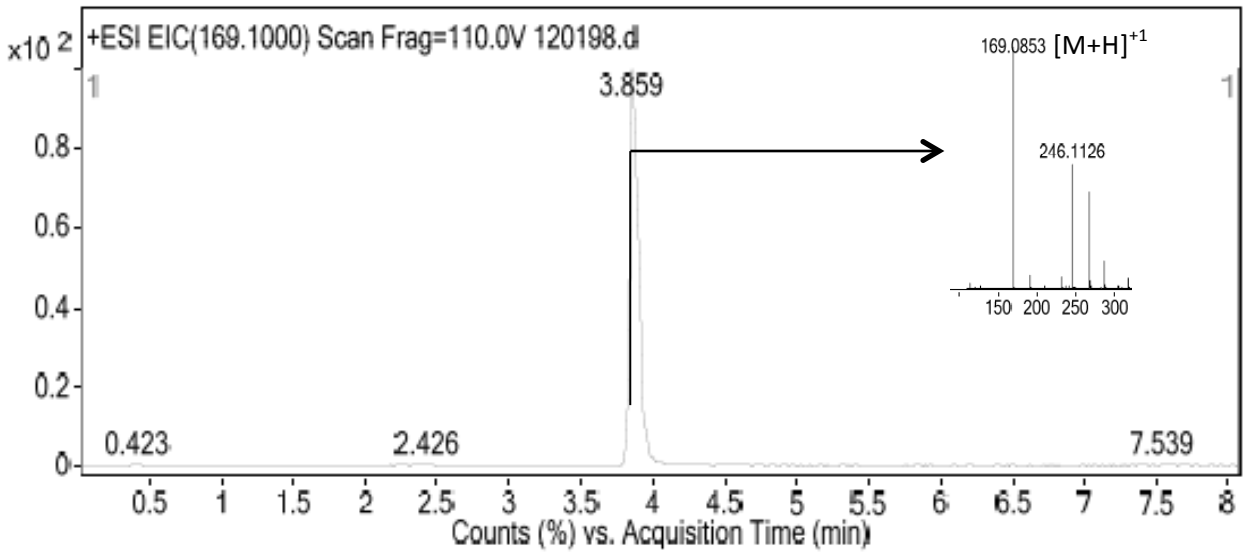

Reaction with 2c

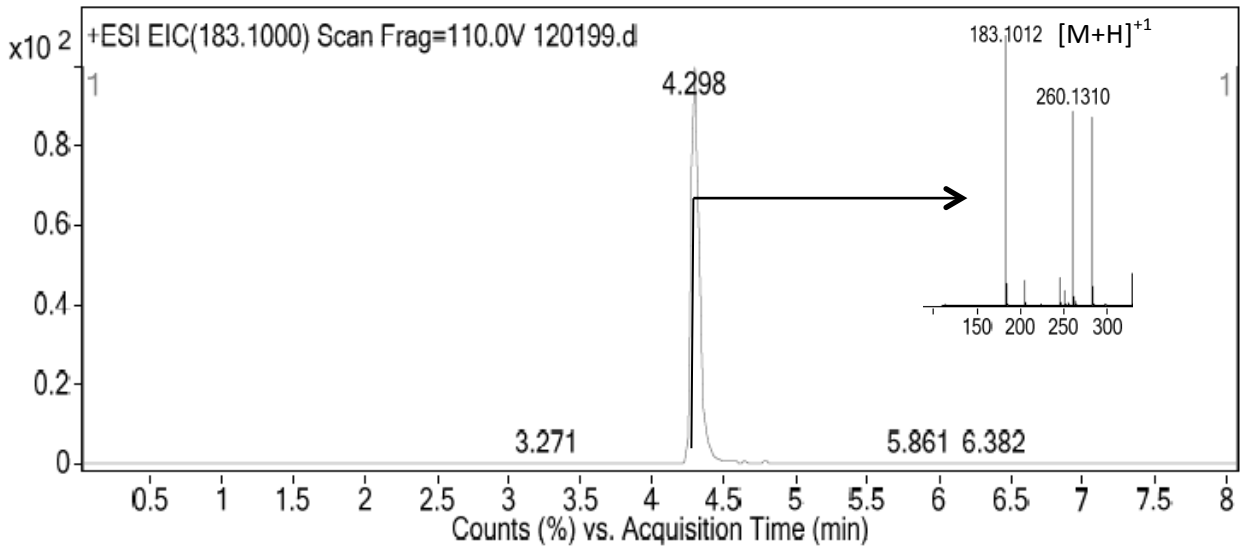

Reaction with 2d

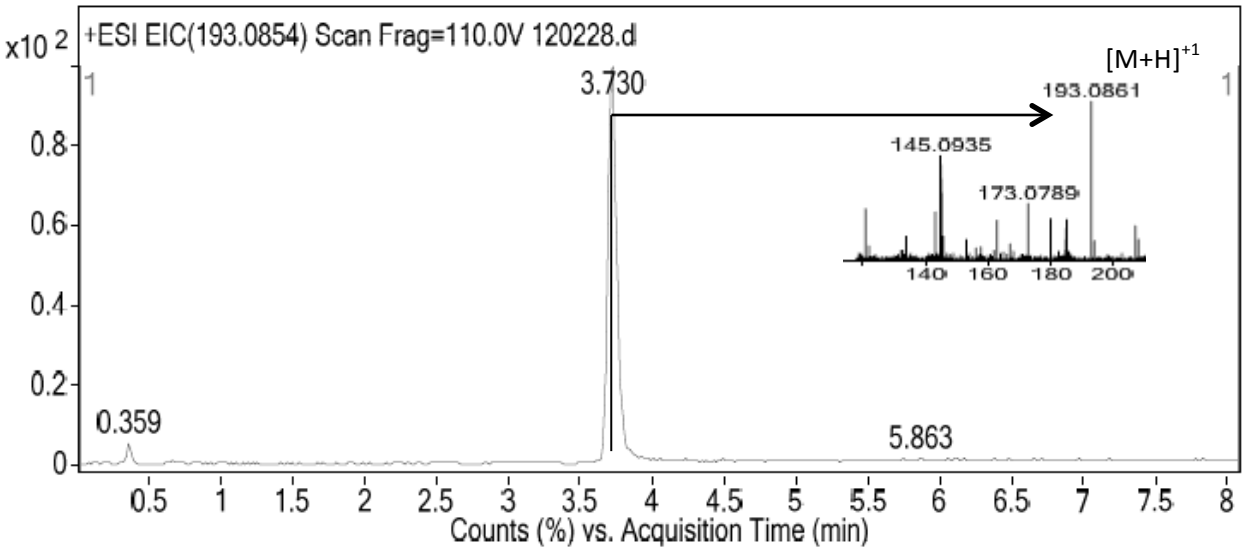

Reaction with 2e

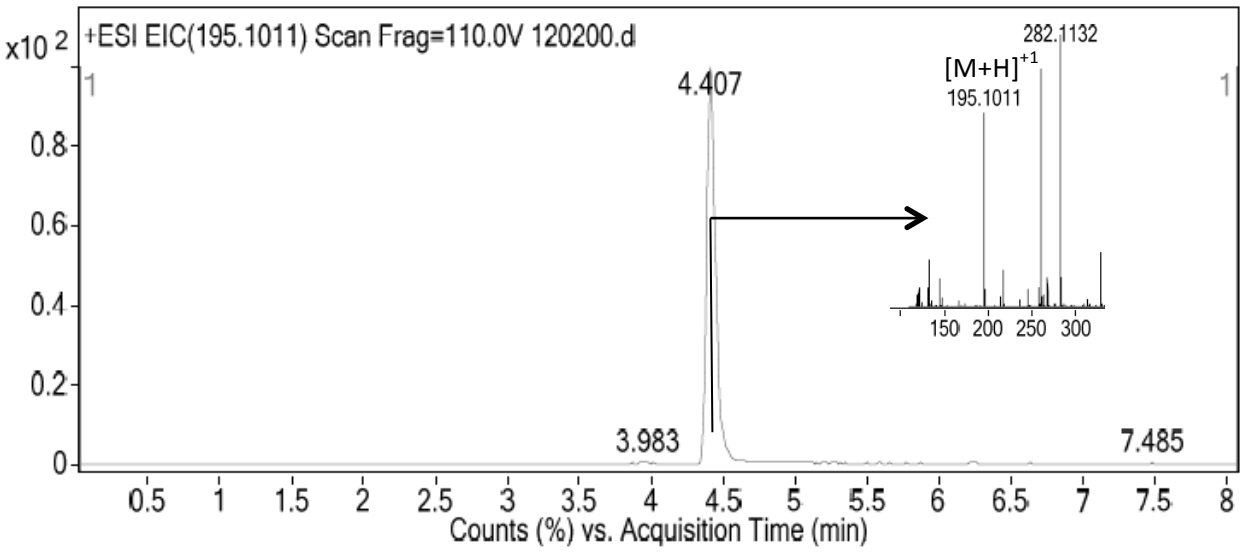

Reaction with 2f

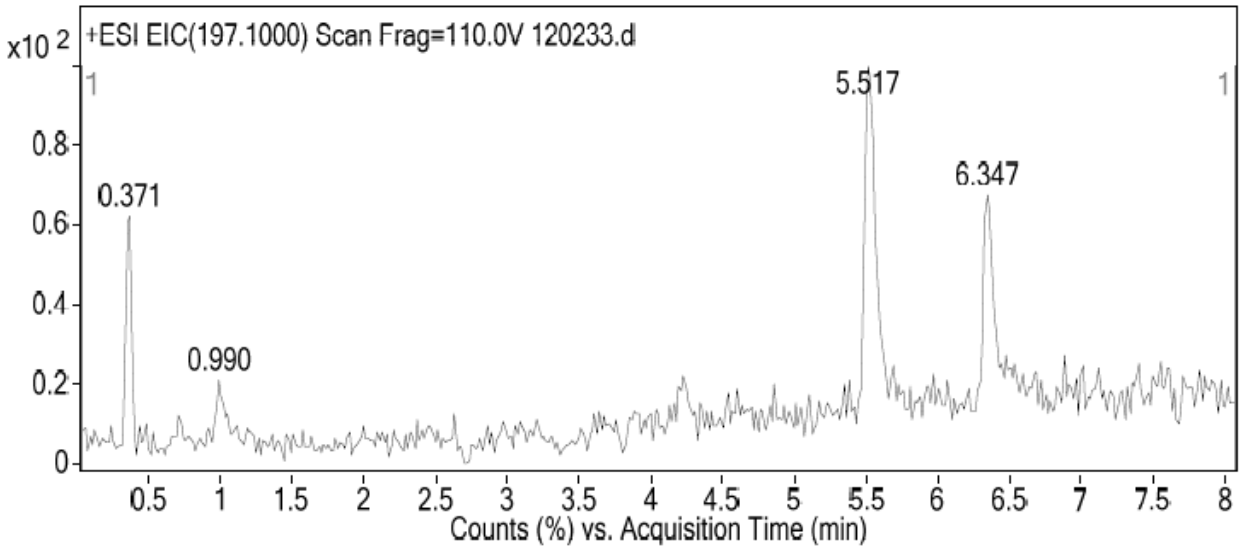

Reaction with 2g

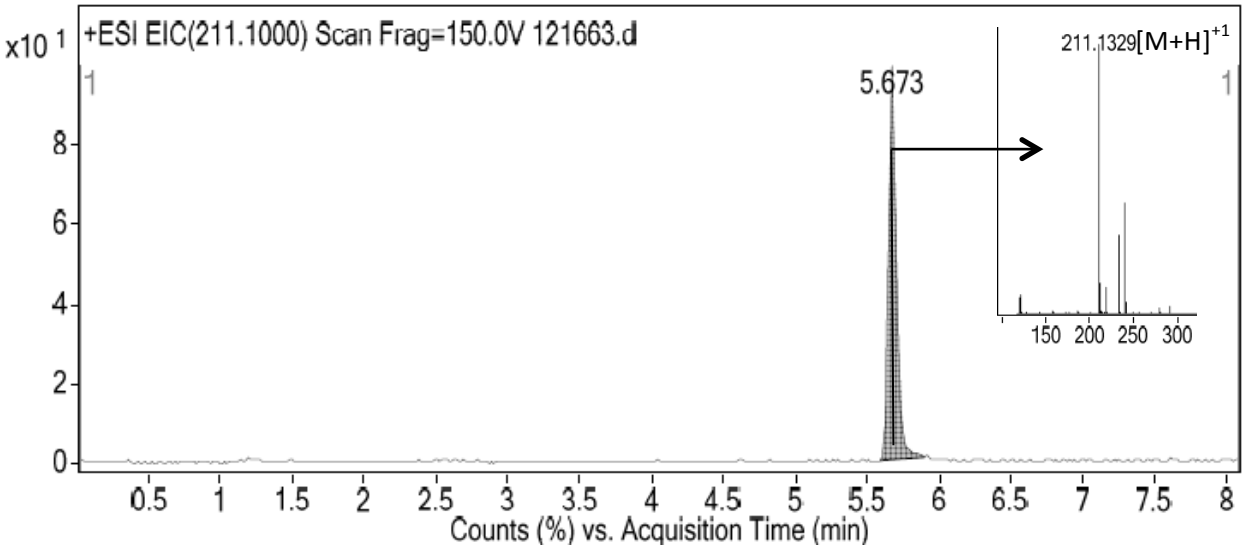

Reaction with 2h

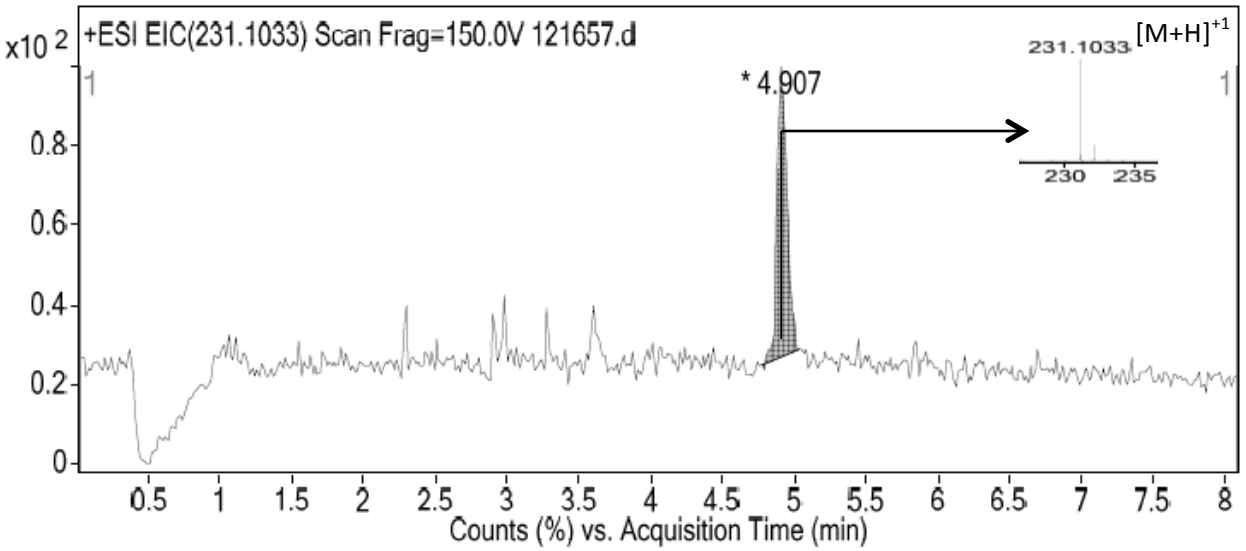

Reaction with 2i

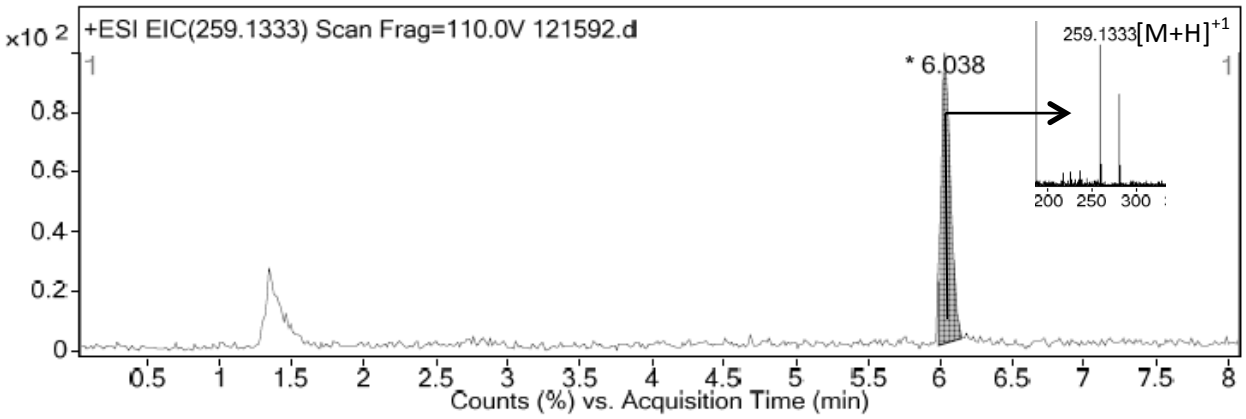

Reaction with 2j

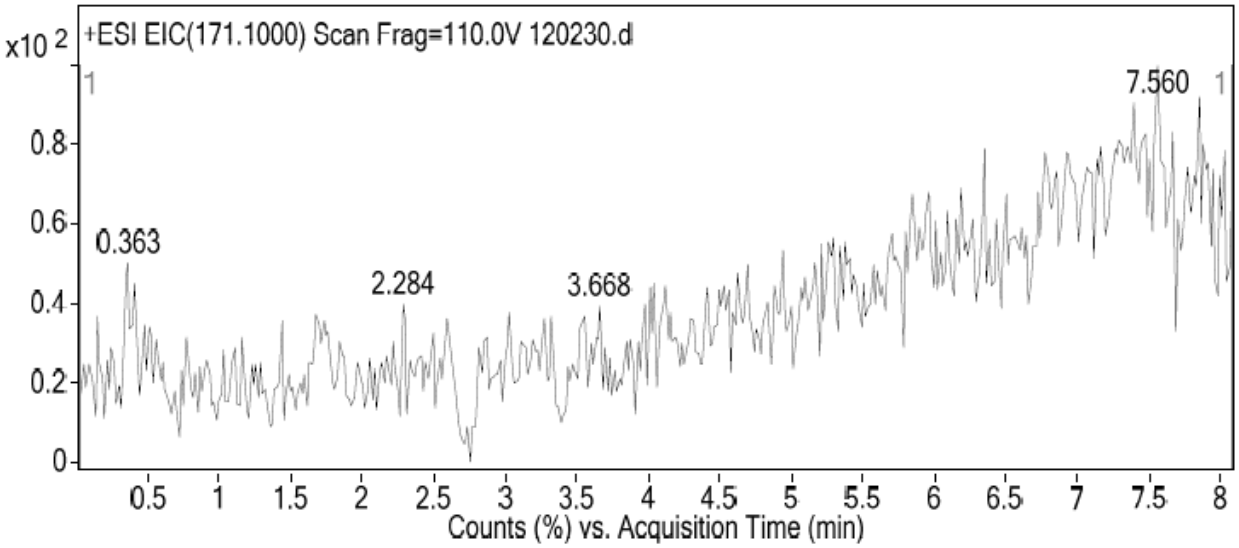

Reaction with 2k

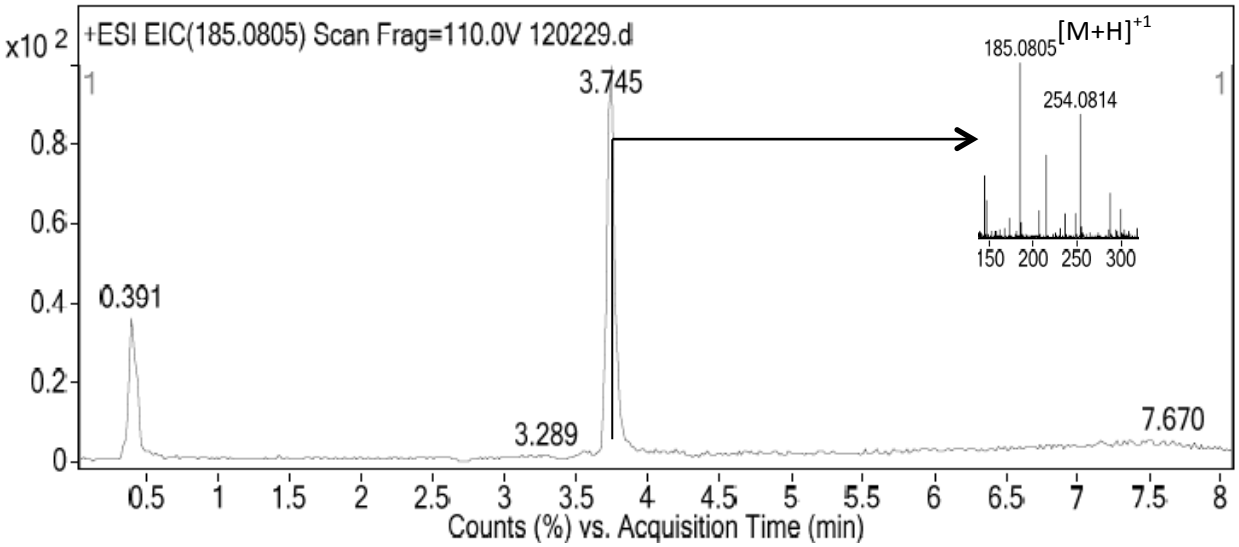

Reaction with 2l

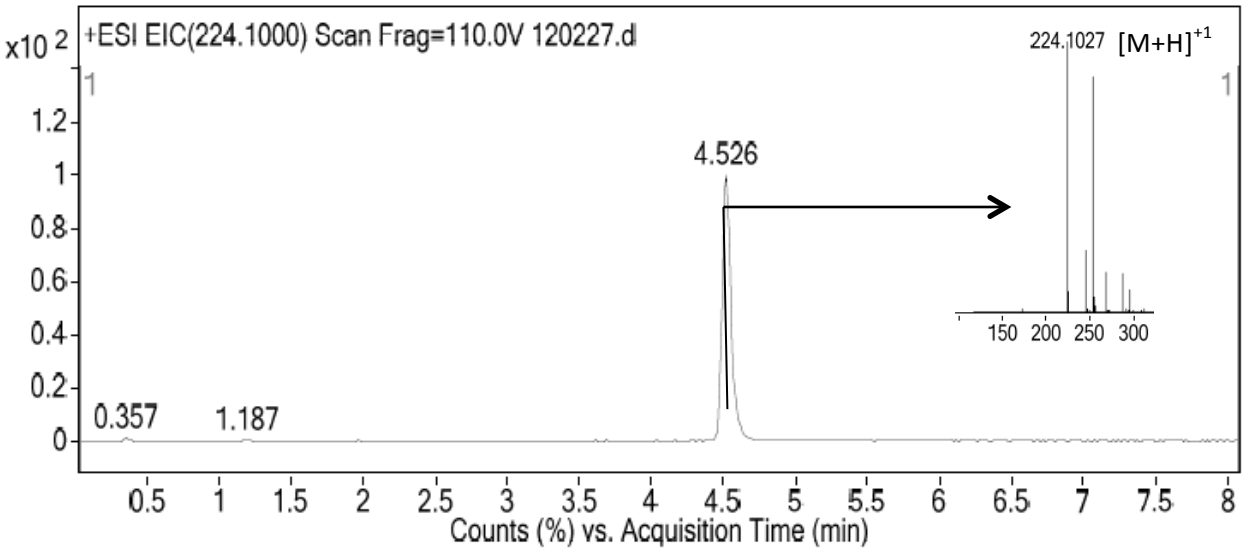

Table S1. RP-HPLC and High-Res LC-MS analysis of *holo*-Mod6TE-catalyzed formation of triketide lactones.

Acyl-CoA/ product[a]	Product retention time (mins)[b]	Relative conversion rate (%)[c]	Calculated mass[d]	Observed mass[e]
2a/3a	N.D[f]	N.D[f]	155.0703	N.D[f]
2b/3b	26.29	100	169.0859	169.0858
2c/3c	31.88	44	183.1016	183.1012
2d/3d	29.31	15	193.0859	193.0861
2e/3e	34.23	36	195.1016	195.1011
2f/3f	N.D[f]	N.D[f]	197.1172	N.D[f]
2g/3g	23.72	1	211.1329	211.1329
2h/3h	N.D[f]	trace	231.1016	231.1044
2i/3i	25.96	2	259.1302	259.1333
2j/3j	N.D[f]	N.D[f]	171.0652	N.D[f]
2k/3k	26.44	9	185.0808	185.0805
2l/3l	37.32	31	224.1030	224.1027

[a] See Scheme 1 for structures of acyl-CoAs and products.
[b] HPLC retention time. See Supplemental Information for HPLC conditions.
[c] Relative conversions were determined by HPLC and calculated by dividing the integrated area of the product from the non-natural acyl-CoA by the integrated area of the product from **2b**. Minimum detection limit is 1.6 % conversion. See Supplemental Information for reaction conditions.
[d] Calculated mass of triketide pyrone product, $[M+H]^+$.
[e] Observed mass of triketide pyrone product, $[M+H]^+$. See Supplemental Information for LC-MS conditions.
[f] N.D, non-detected.

Figure S2. RP-HPLC analysis of *holo*-Mod6TE negative control reactions using the extender units (i) **2a**, (ii) **2b**, (iii) **2c**, (iv) **2d**, (v) **2e**, (vi) **2f**, (vii) **2g**, (viii) **2h**, (ix) **2i**, (x) **2j**, (xi) **2k**, (xii) **2l**. Panel (a) are negative control reactions that lacked *holo*-Mod6TE. Panel (b) are negative control reactions that lacked diketide-SNAc **4**. * indicates contaminants present in the **2g**-**2i** acyl-CoA preparations which were detected under the specialized conditions required for HPLC analysis of the resulting lactones. Each sample was also analyzed by low res ESI-MS (Table S3). See Supplemental Information for assay conditions and detection methods.

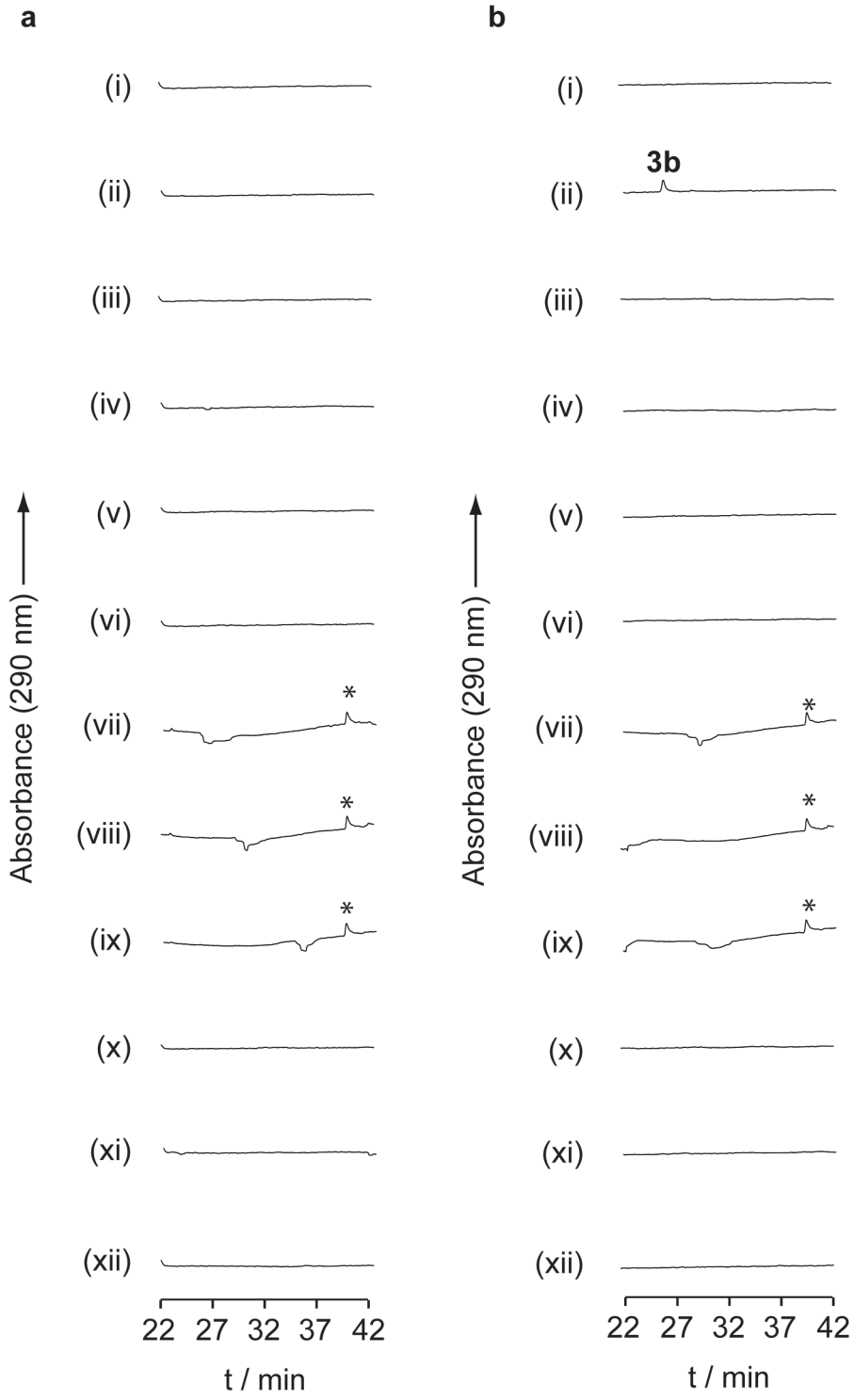

Table S2. RP-HPLC and Low Res ESI-MS analysis of *holo*-Mod6TE negative control reactions that lack diketide-SNAc **4**.

Acyl-CoA/ product[a]	Product retention time (mins)[b]	Relative conversion rate (%)[c]	Calculated mass[d]	Observed Mass[e]
2a/3a	N.D[f]	N.D[f]	155.07	N.D[f]
2b/3b	26.29	7.1[f]	169.08	169.10
2c/3c	N.D[f]	N.D[f]	183.10	N.D[f]
2d/3d	N.D[f]	N.D[f]	193.08	N.D[f]
2e/3e	N.D[f]	N.D[f]	195.10	N.D[f]
2f/3f	N.D[f]	N.D[f]	197.1011	N.D[f]
2g/3g	N.D[f]	N.D[f]	211.13	N.D[f]
2h/3h	N.D[f]	N.D[f]	231.10	N.D[f]
2i/3i	N.D[f]	N.D[f]	259.13	N.D[f]
2j/3j	N.D[f]	N.D[f]	171.06	N.D[f]
2k/3k	N.D[f]	N.D[f]	185.08	N.D[f]
2l/3l	N.D[f]	N.D[f]	224.10	N.D[f]

[a] See Scheme 1 for structures of acyl-CoAs and products.
[b] HPLC retention time/Low Res LC-MS retention time. See Supplemental Information for HPLC and LC-MS conditions.
[c] Calculated mass of triketide pyrone product, $[M+H]^+$.
[d] Relative conversions were determined by HPLC and calculated by dividing the integrated area of the product in the absence of **4** by the integrated area of the same product in the presence of **4** (Table S1). See Supplemental Information for reaction conditions.
[e] Observed mass of triketide pyrone product, $[M+H]^+$.
[f] N.D, non-detected.

Figure S3. ^{1}H-NMR of the methyl triketide pyrone **3b**.

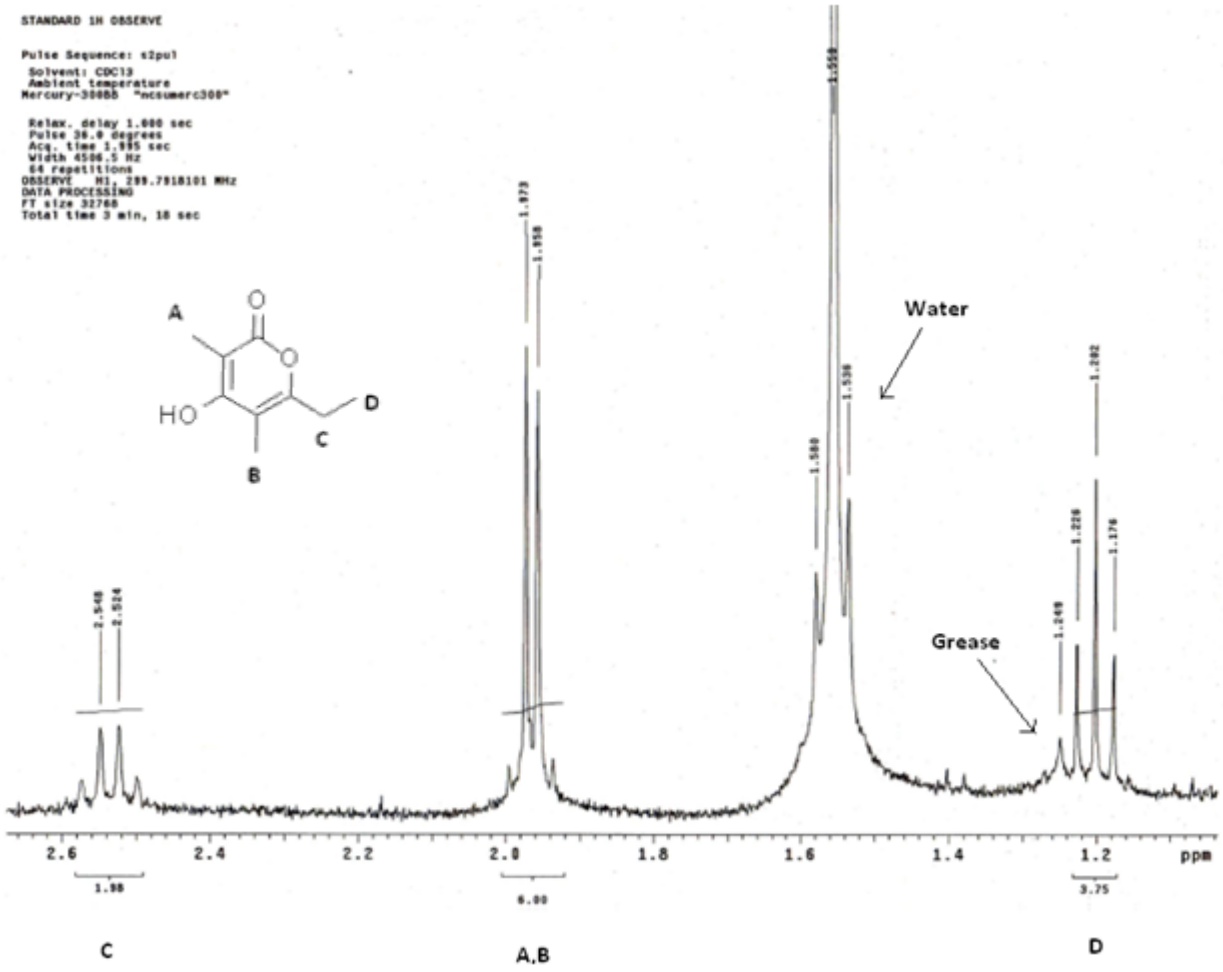

Figure S4. ^{1}H-NMR of the allyl triketide pyrone **3e**.

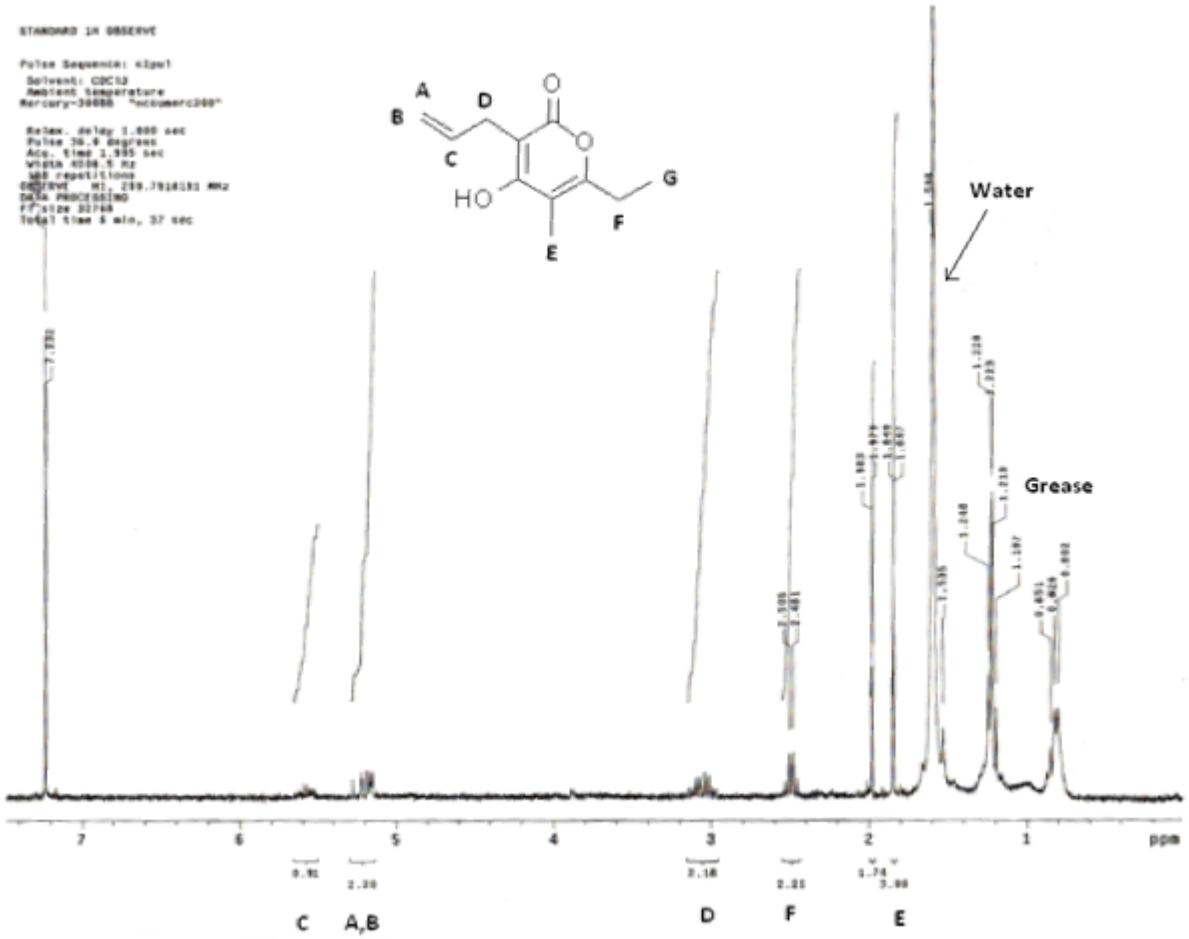

Figure S5. HPLC calibration curve of the methyl triketide pyrone **3b**.

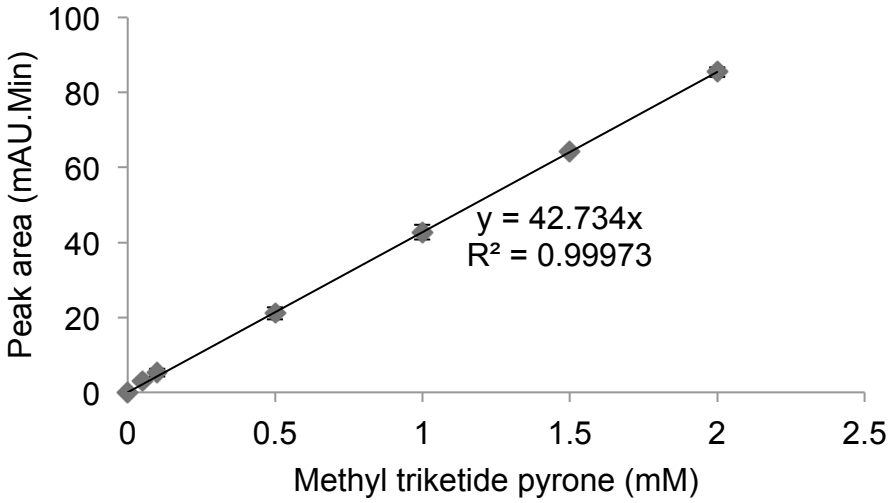

Figure S6. RP-HPLC analysis of *holo*-AT^{o}-Mod6TE reactions using the diketide-SNAc **4** and each extender unit (i) **2a**, (ii) **2b**, (iii) **2c**, (iv) **2d**, (v) **2e**, (vi) **2f**, (vii) **2g**, (viii) **2h**, (ix) **2i**, (x) **2j**, (xi) **2k**, (xii) **2l**. Mass ions consistent with the expected triketide lactone were not observed for **2a**-**f** and **2j**-**l** (data not shown). For **2g**, **2h**, and **2i**, very low abundance mass ions (211.10, 231.10 and 259.10 respectively, data not shown) were observed that were in agreement with the expected lactone. * indicates contaminants present in the **2g**-**2i** acyl-CoA preparations which were detected under the specialized conditions required for HPLC analysis of the resulting lactones. See Supplemental Information for assay conditions and detection methods.

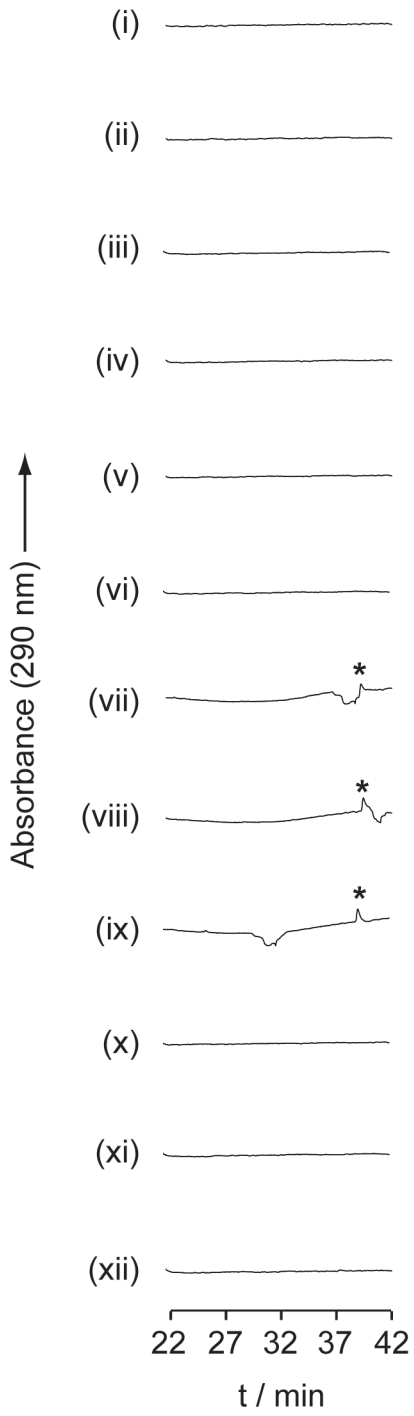

Figure S7. RP-HPLC analysis of the conversion of *apo*-AT^{o}-Mod6TE to triketide lactone using each extender unit in the absence of Sfp (i) **2a**, (ii) **2b**, (iii) **2c**, (iv) **2d**, (v) **2e**, (vi) **2f**, (vii) **2g**, (viii) **2h**, (ix) **2i**, (x) **2j**, (xi) **2k**, (xii) **2l**. For **2g**, **2h**, and **2i**, very low abundance mass ions (211.10, 231.10 and 259.10 respectively, data not shown) were observed that were in agreement with the expected lactone.* indicates contaminants present in the **2g**-**2i** acyl-CoA preparations which were detected under the specialized conditions required for HPLC analysis of the resulting lactones. See Supplemental Information for assay conditions and detection methods.

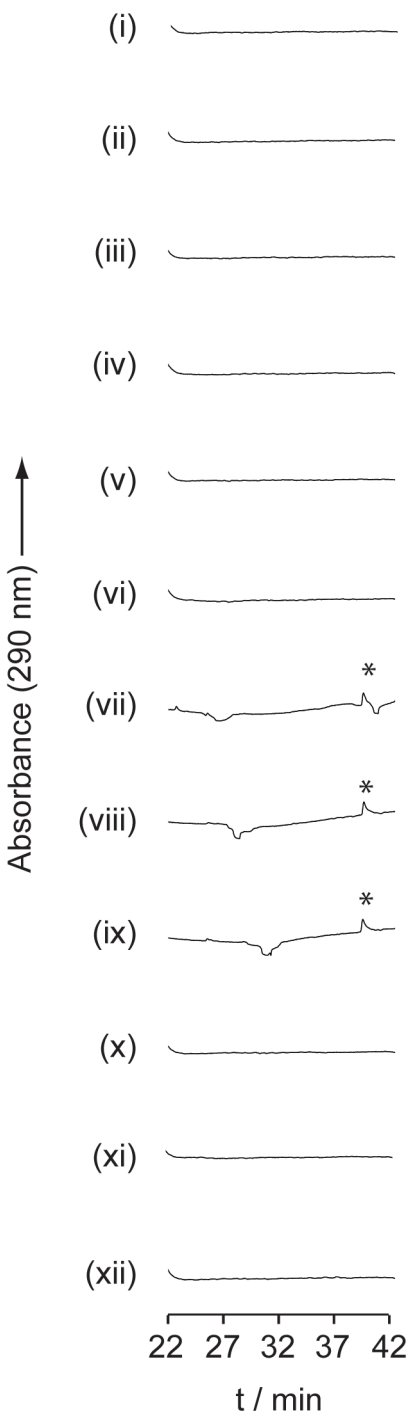

Figure S8. LC-MS analysis of Sfp-catalyzed acylation of *apo*-ACP6 from DEBS. A control reaction (L) that lacks any acyl-CoA is included to demonstrate identification of acylated ACP is dependent on the presence of extender unit. A series of negative controls that lacked Sfp are included (M-W) and illustrate that Sfp is absolutely required to acylate the ACP. See Supplemental Information for assay conditions and detection methods.

A) Sfp loading of DEBS *apo*-ACP6 with 2a produced by WT-MatB

***Deconvoluted spectra*:**

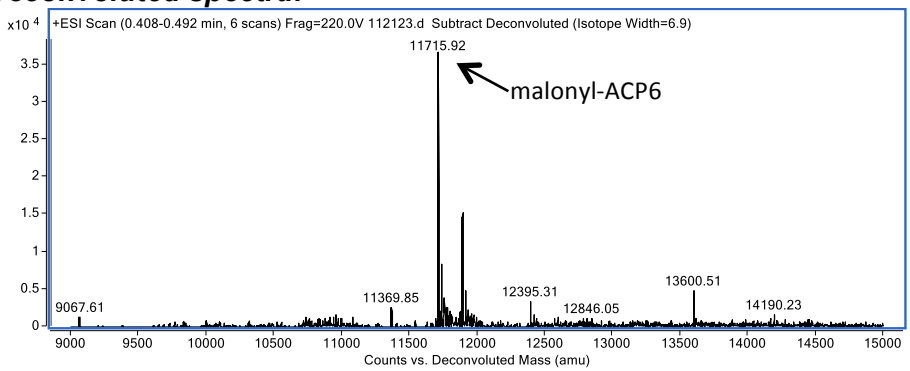

***Deconvoluted spectra, expanded on target peak*:**

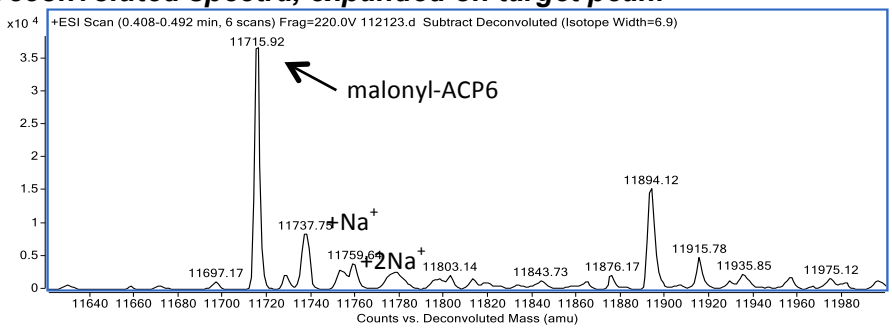

***Component m/z*:**

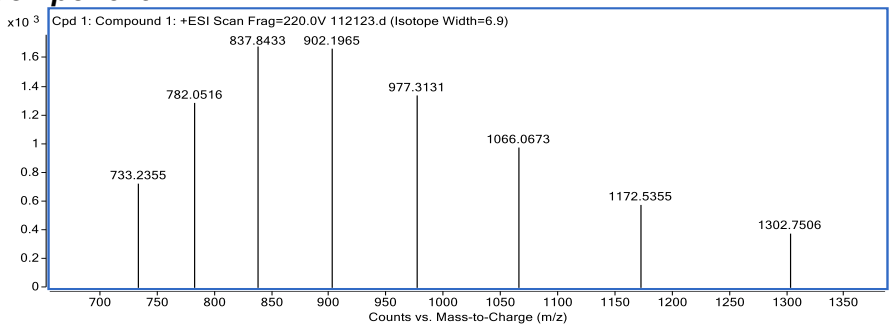

***Component charge state*:**

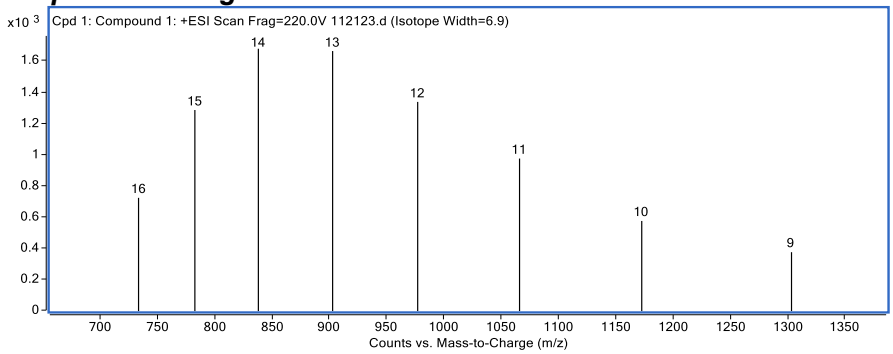

B) Sfp loading of DEBS *apo*-ACP6 with 2b produced by WT-MatB

Deconvoluted spectra:

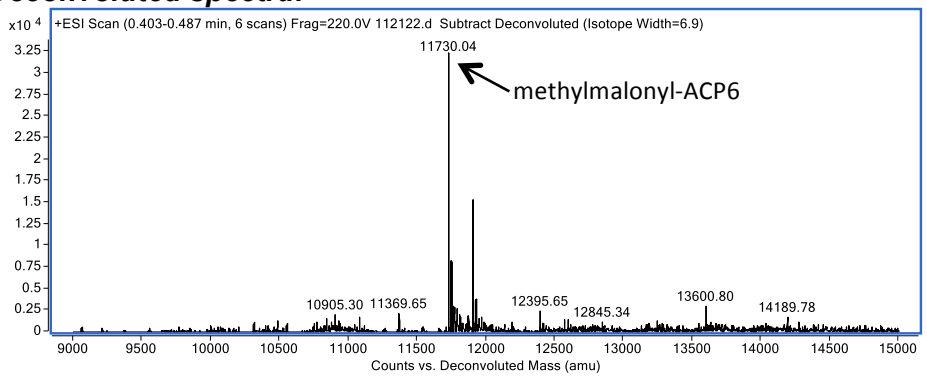

Deconvoluted spectra, expanded on target peak:

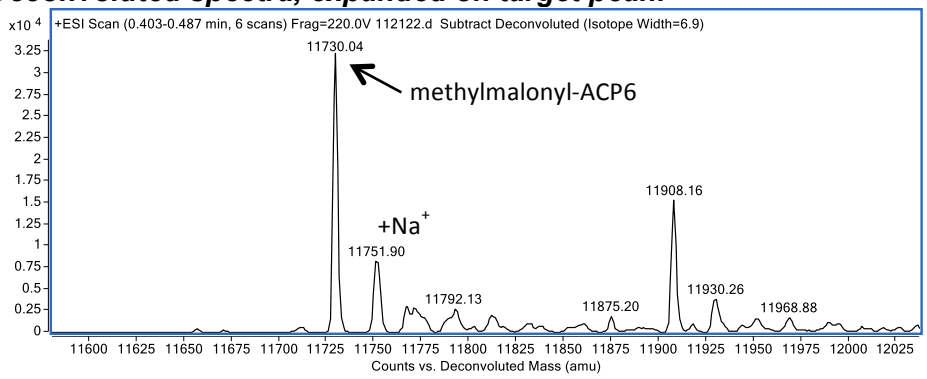

Component m/z:

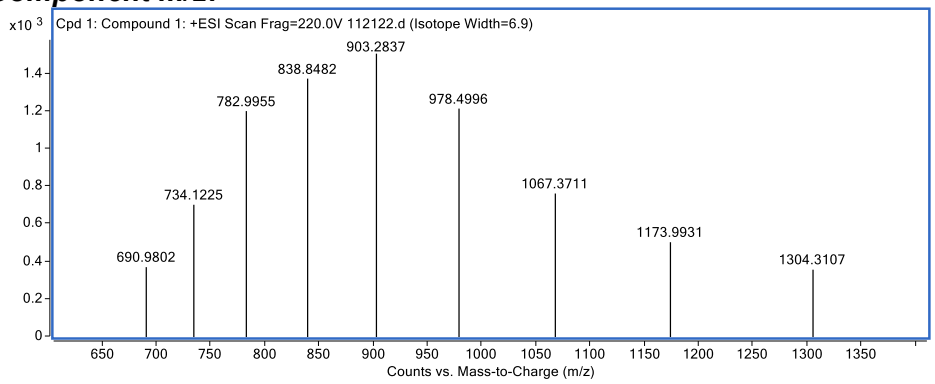

Component charge state:

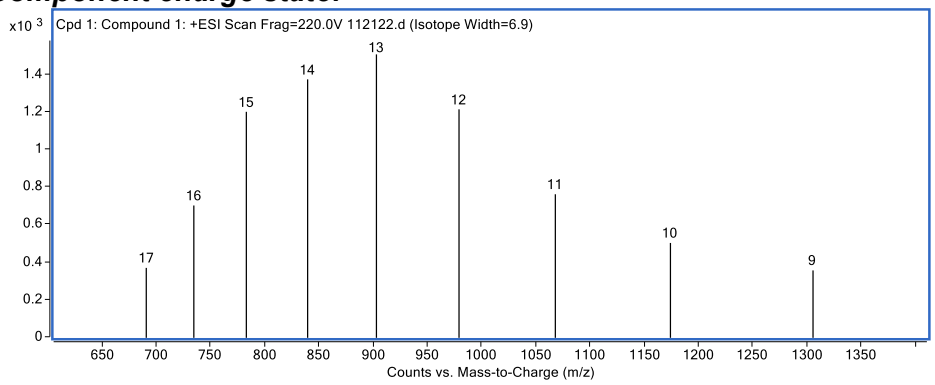

C) Sfp loading of DEBS *apo*-ACP6 with 2c produced by MatB T207S/M306I

Deconvoluted spectra:

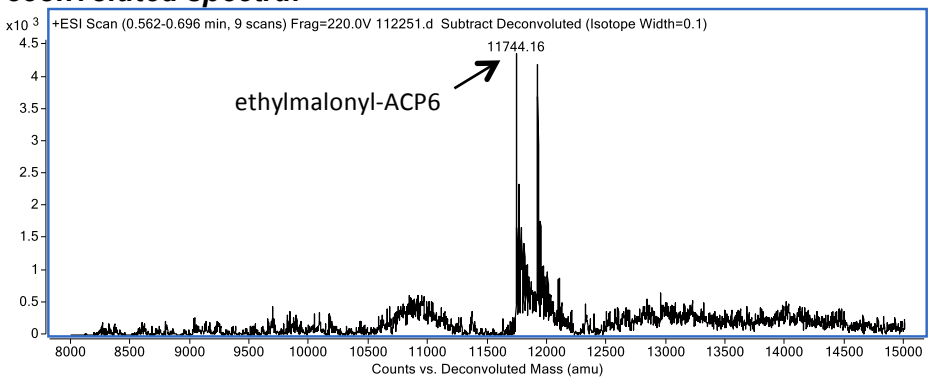

Deconvoluted spectra, expanded on target peak:

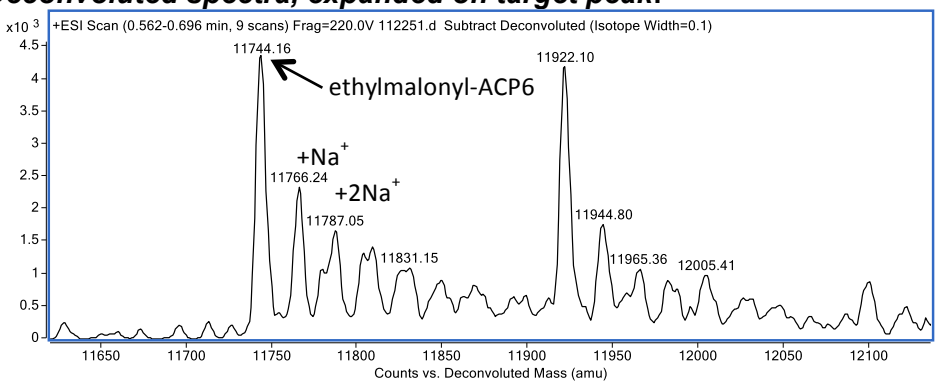

Component m/z:

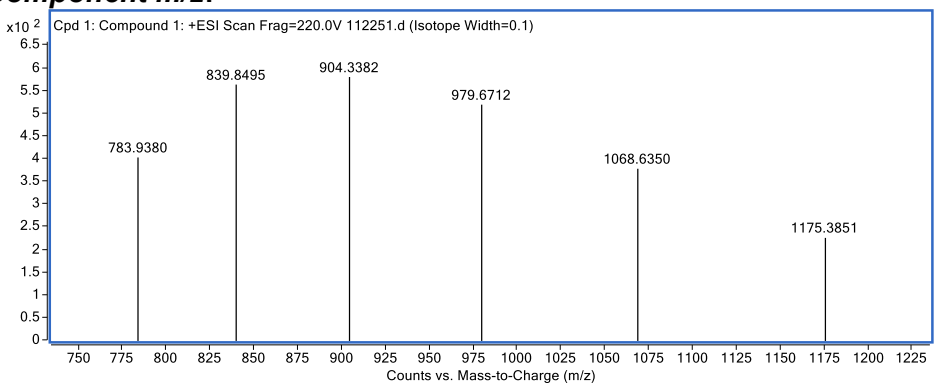

Component charge state:

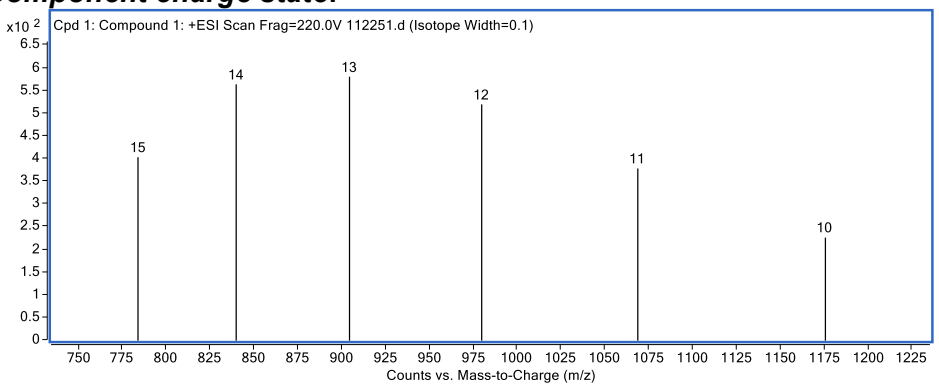

D) Sfp loading of DEBS *apo*-ACP6 with 2d produced by MatB T207G/M306I

Deconvoluted spectra:

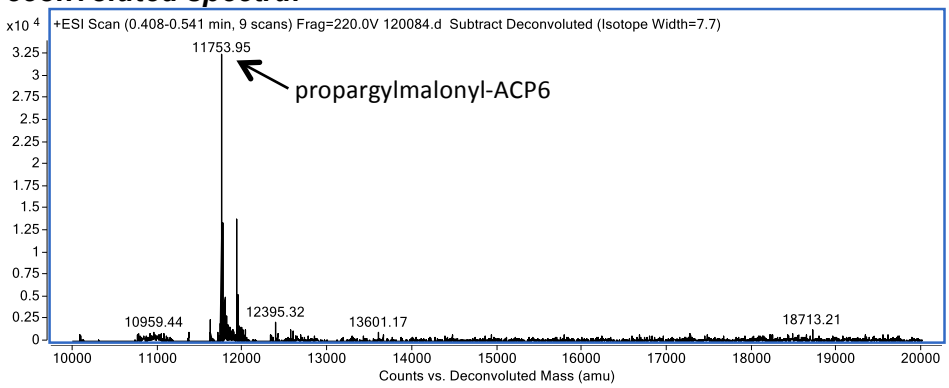

Deconvoluted spectra, expanded on target peak:

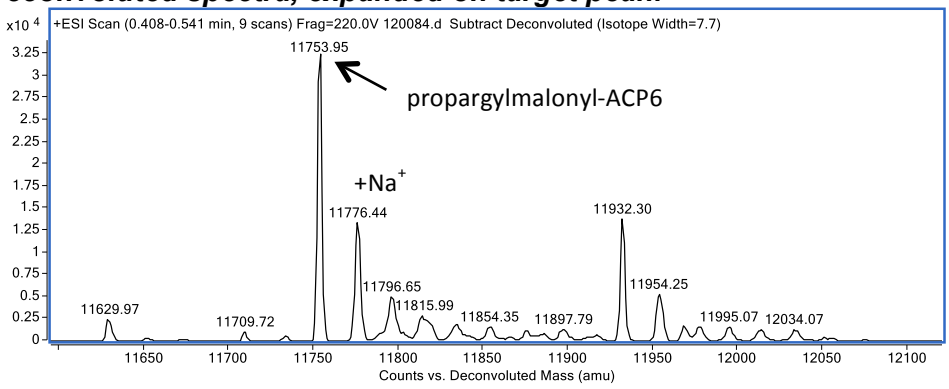

Component m/z:

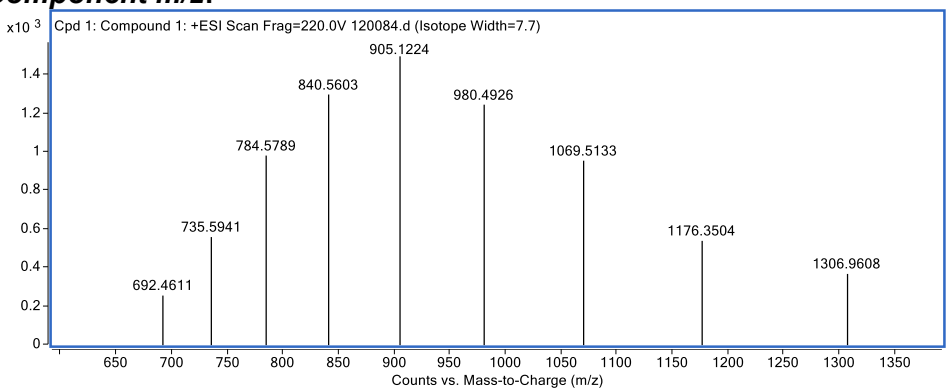

Component charge state:

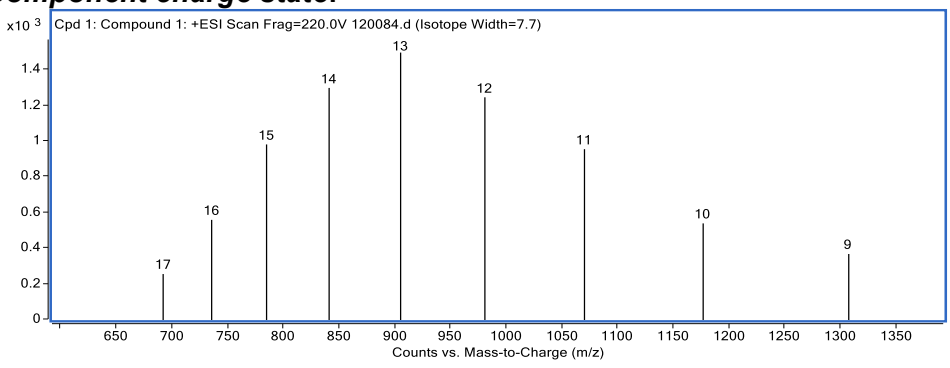

E) Sfp loading of DEBS *apo*-ACP6 with 2e produced by MatB T207S/M306I

Deconvoluted spectra:

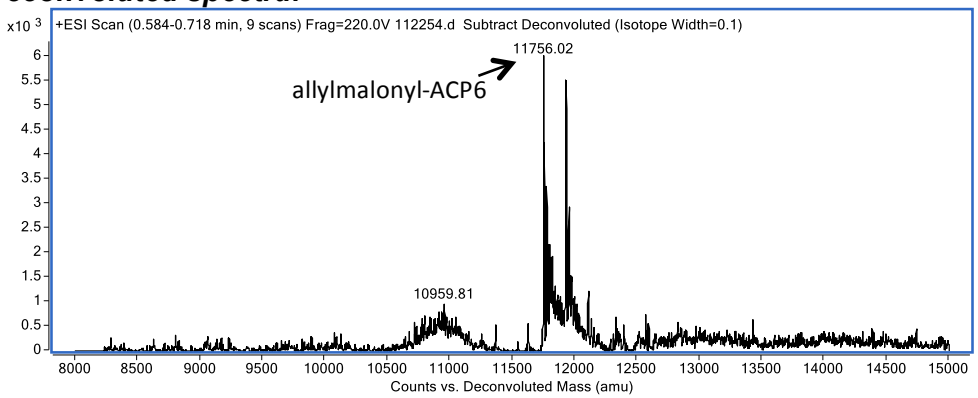

Deconvoluted spectra, expanded on target peak:

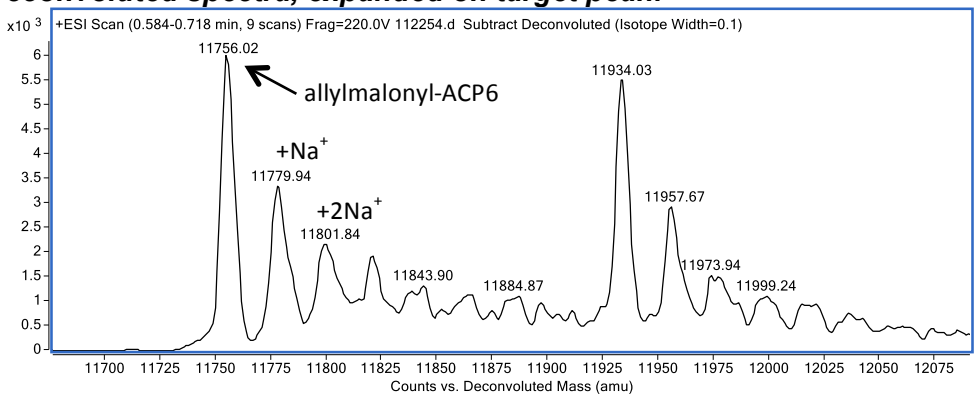

Component m/z:

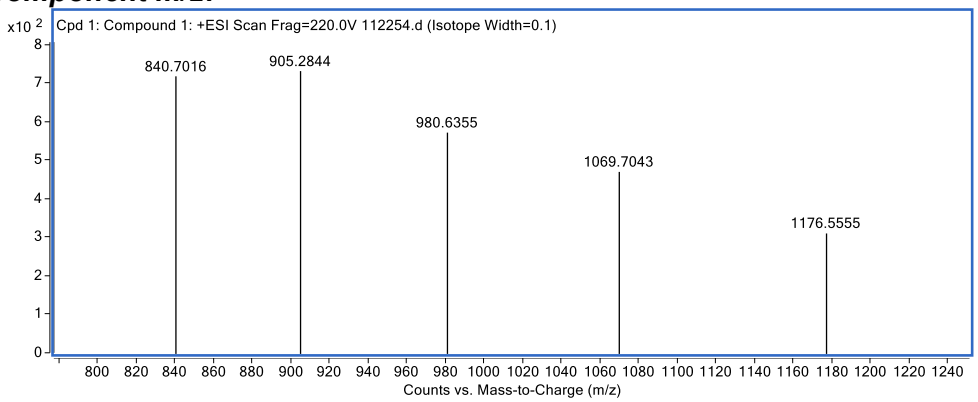

Component charge state:

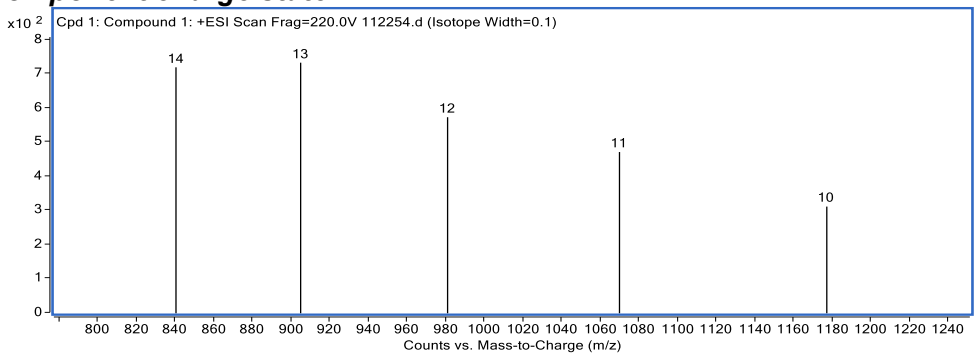

F) Sfp loading of DEBS *apo*-ACP6 with 2f produced by MatB T207G/M306I

Deconvoluted spectra:

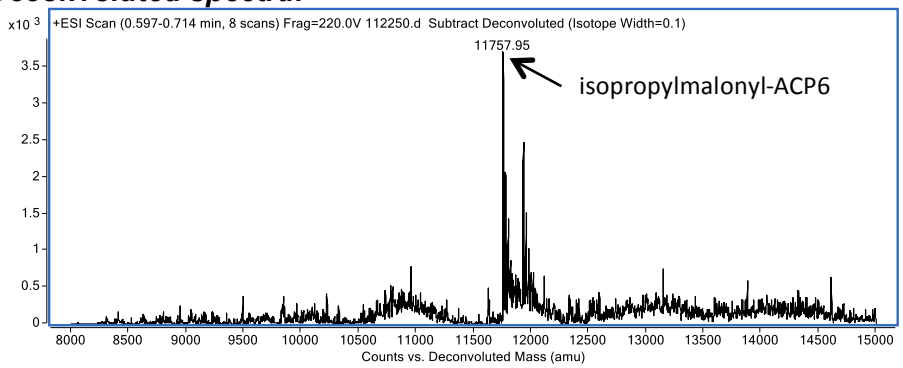

Deconvoluted spectra, expanded on target peak:

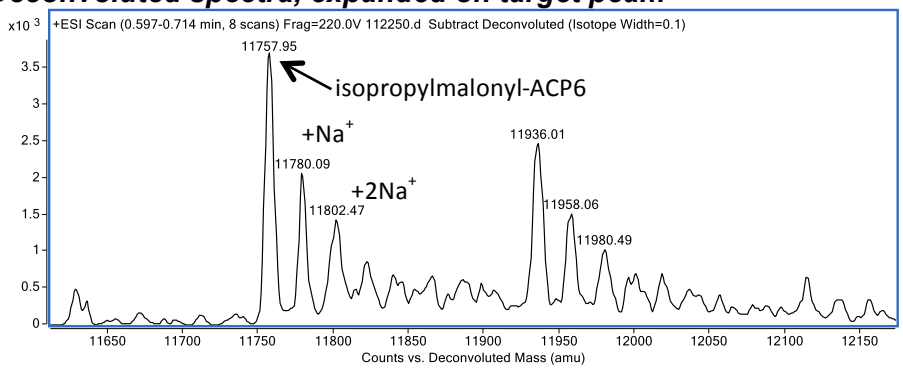

Component m/z:

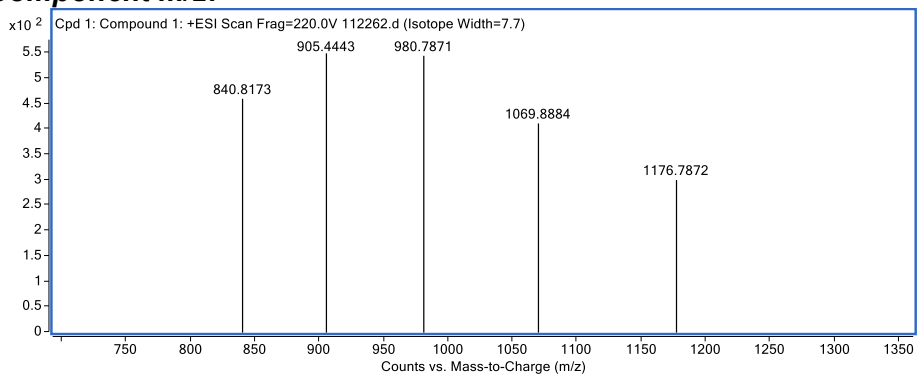

Component charge state:

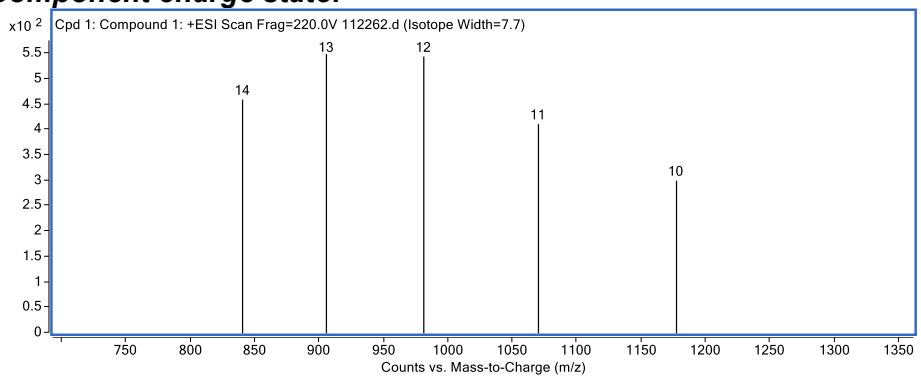

G) Sfp loading of DEBS *apo*-ACP6 with 2g produced by MatB T207A

Deconvoluted spectra:

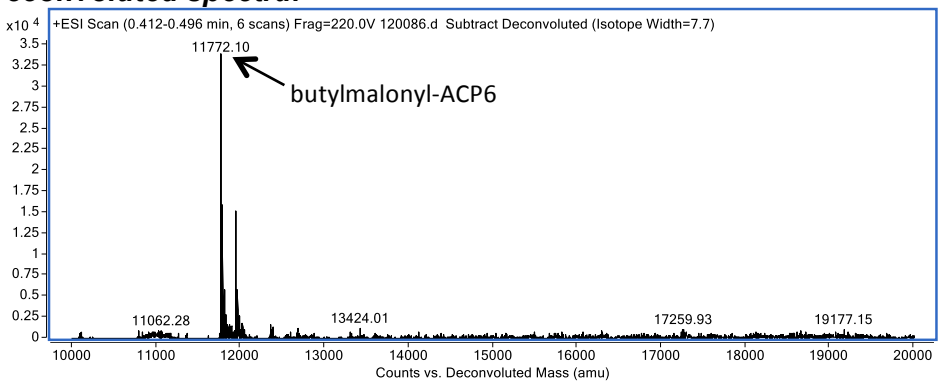

Deconvoluted spectra, expanded on target peak:

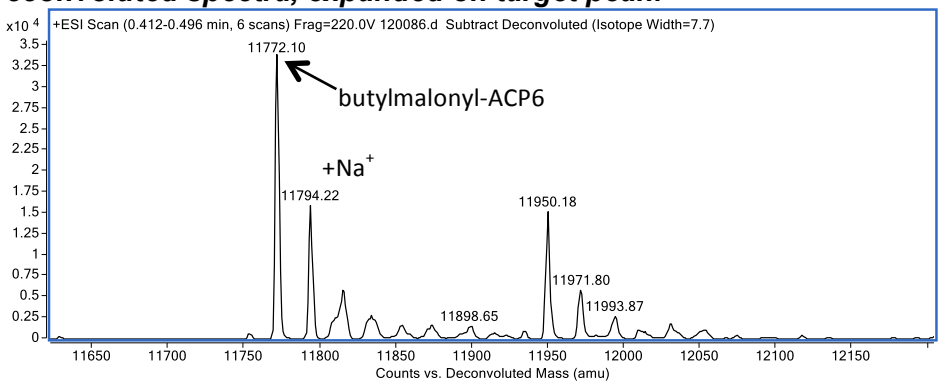

Component m/z:

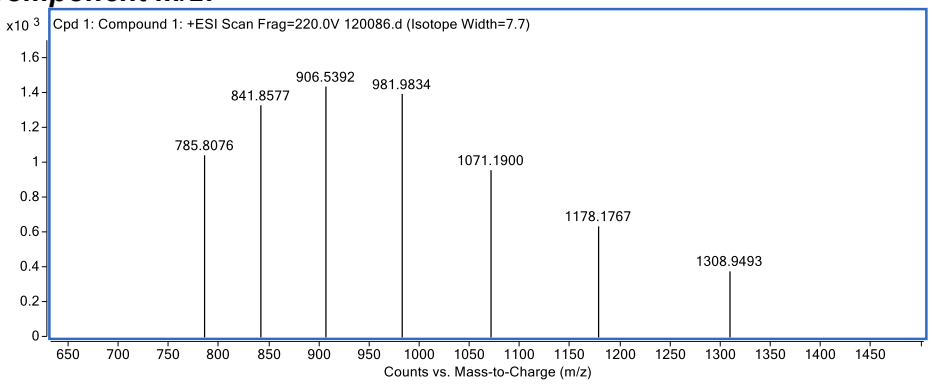

Component charge state:

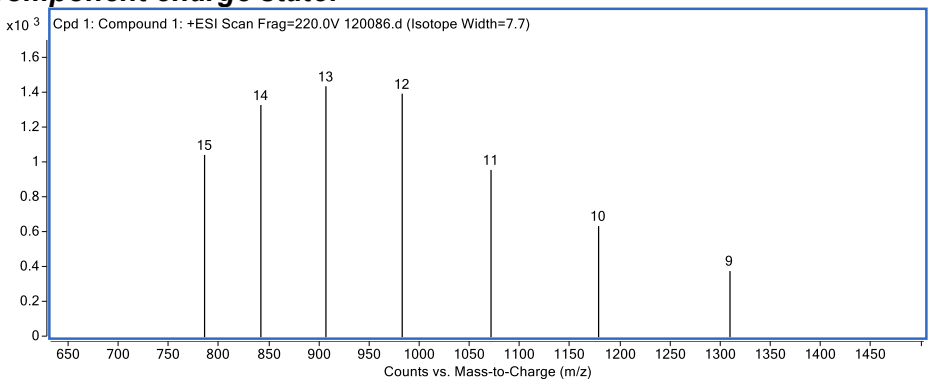

H) Sfp loading of DEBS *apo*-ACP6 with 2h produced by MatB T207G/M306I

Deconvoluted spectra:

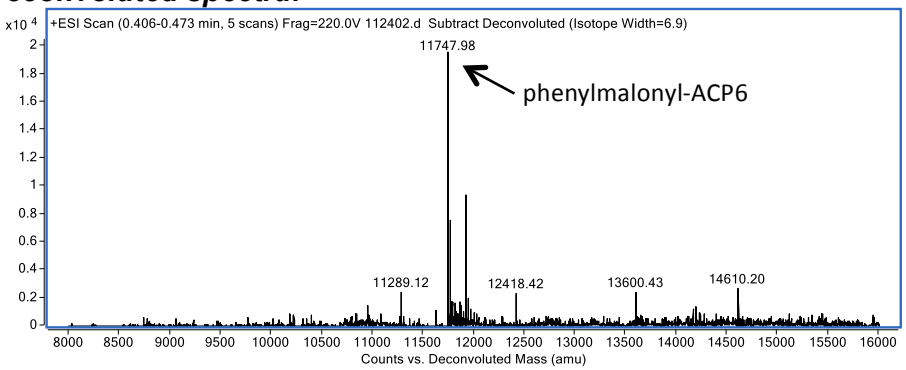

Deconvoluted spectra, expanded on target peak:

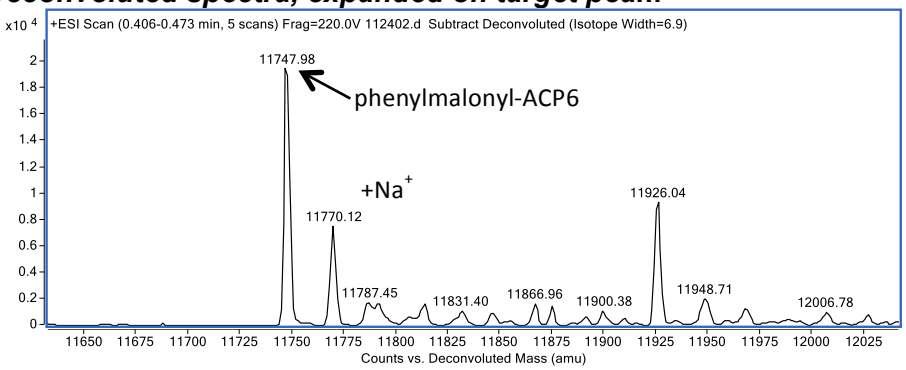

Component m/z:

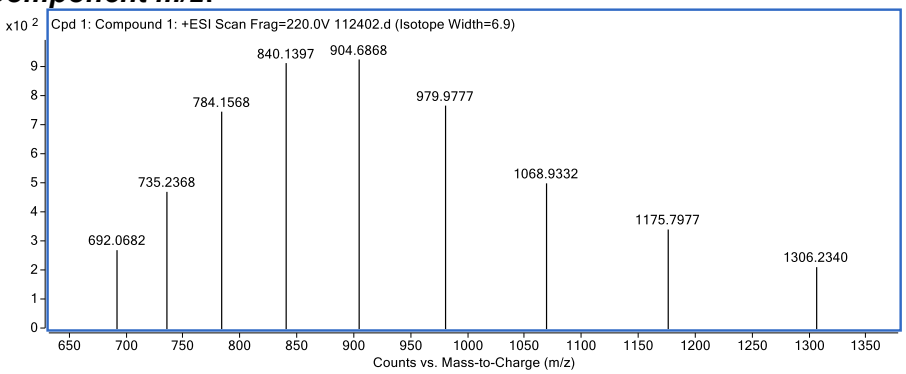

Component charge state:

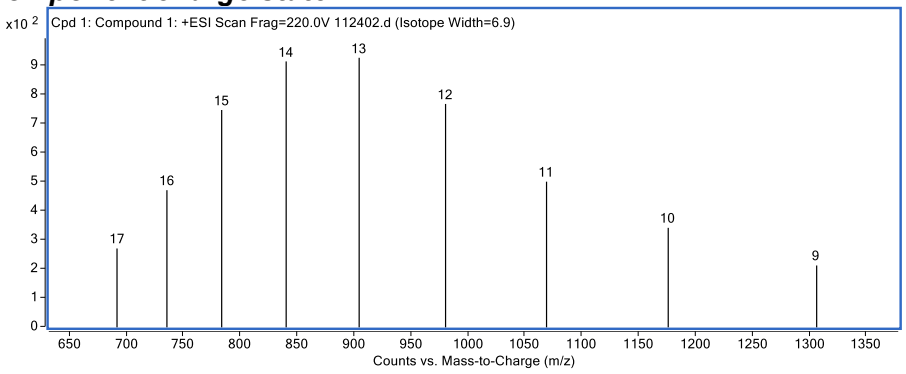

l) Sfp loading of DEBS *apo*-ACP6 with 2i produced by MatB T207G/M306I

***Deconvoluted spectra*:**

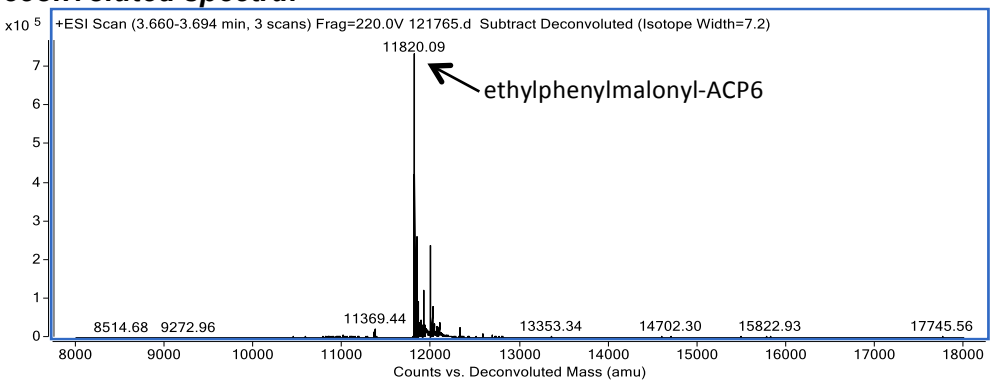

***Deconvoluted spectra, expanded on target peak*:**

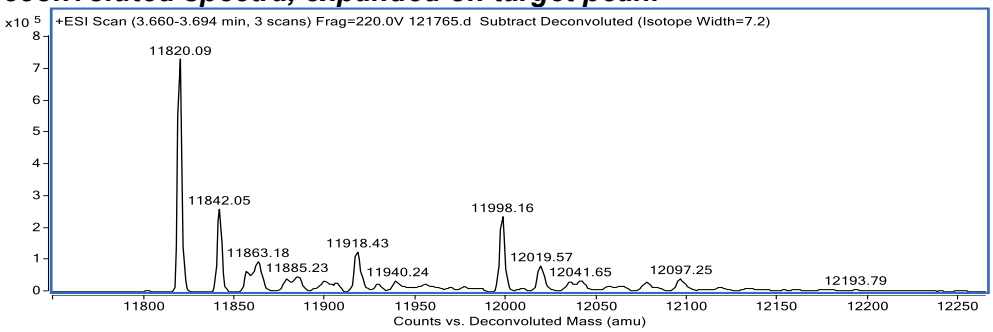

***Component m/z*:**

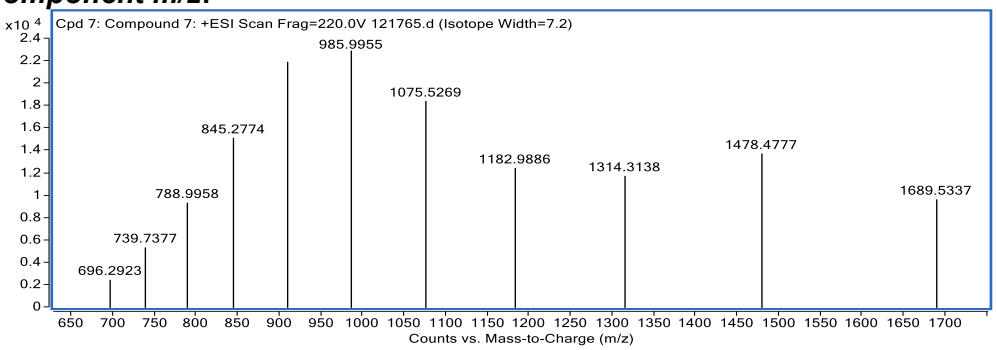

***Component charge state*:**

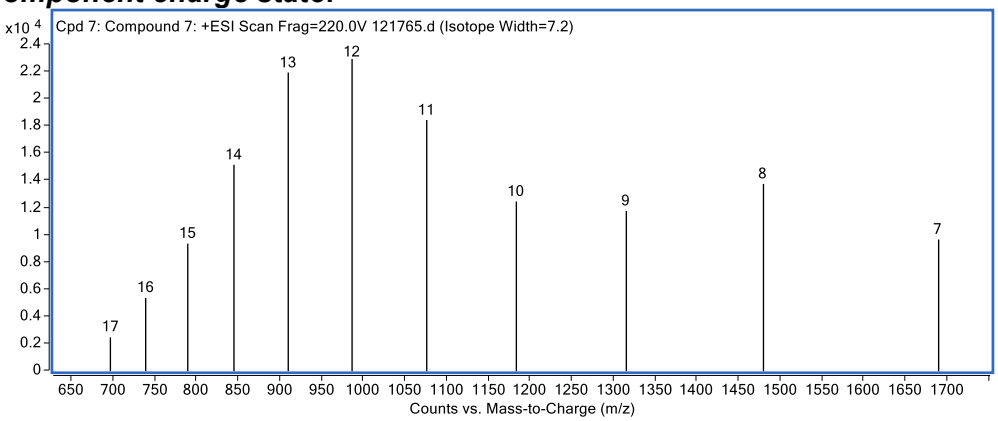

J) Sfp loading of DEBS *apo*-ACP6 with 2j produced by WT MatB

***Deconvoluted spectra*:**

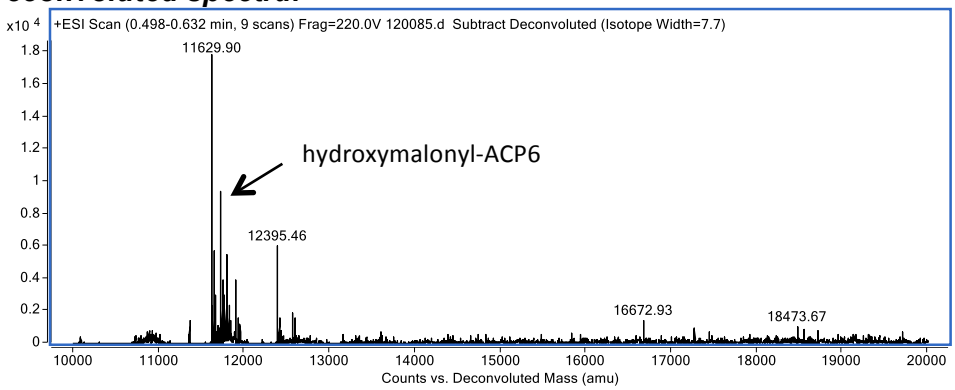

***Deconvoluted spectra, expanded on target peak*:**

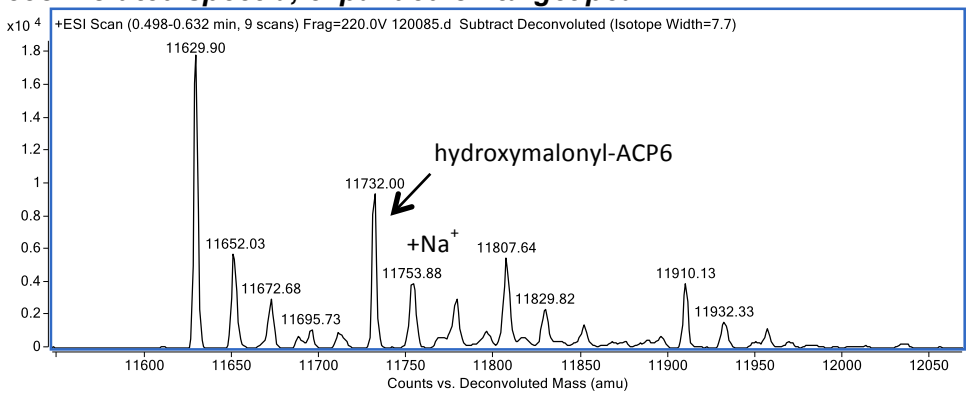

***Component m/z*:**

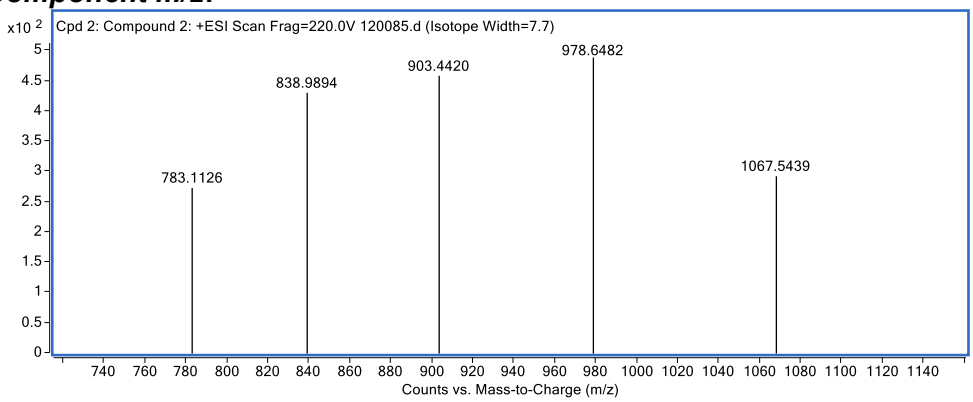

***Component charge state*:**

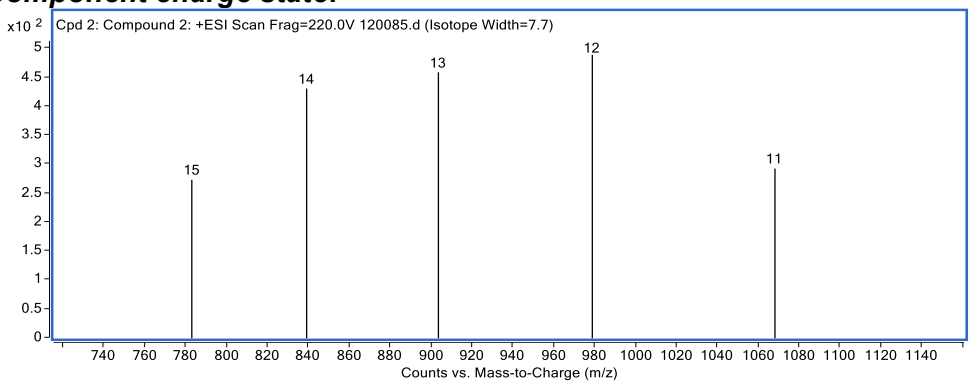

K) Sfp loading of DEBS *apo*-ACP6 with 2k produced by MatB T207A/M306I

Deconvoluted spectra:

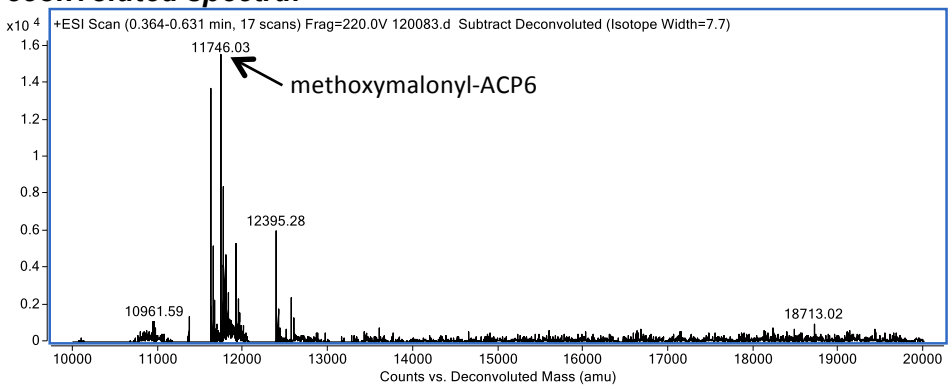

Deconvoluted spectra, expanded on target peak:

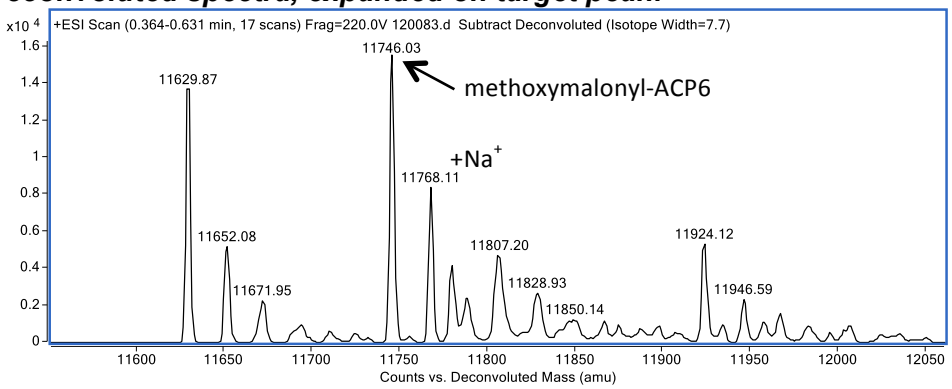

Component m/z:

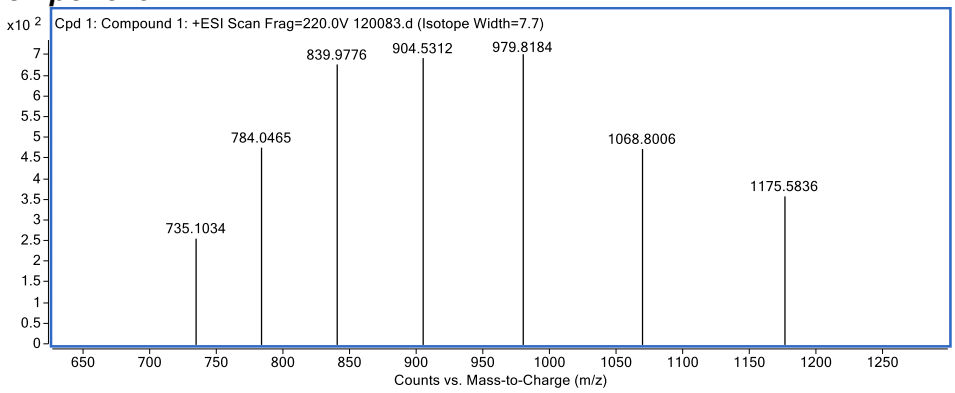

Component charge state:

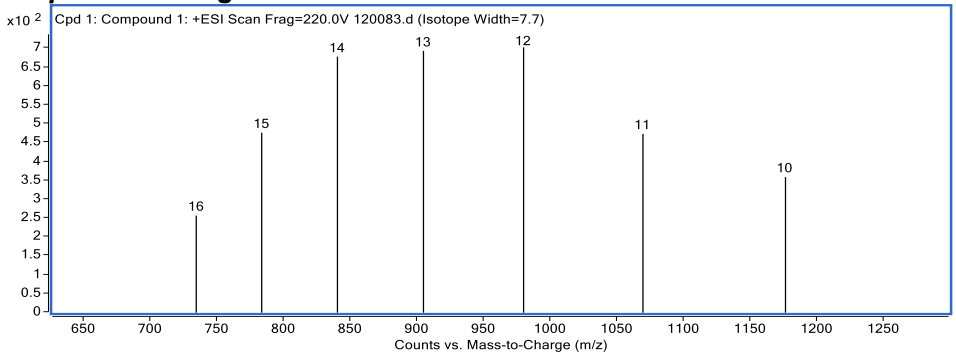

L) Sfp loading of DEBS *apo*-ACP6 with 2l produced by MatB T207G/M306V

Deconvoluted spectra:

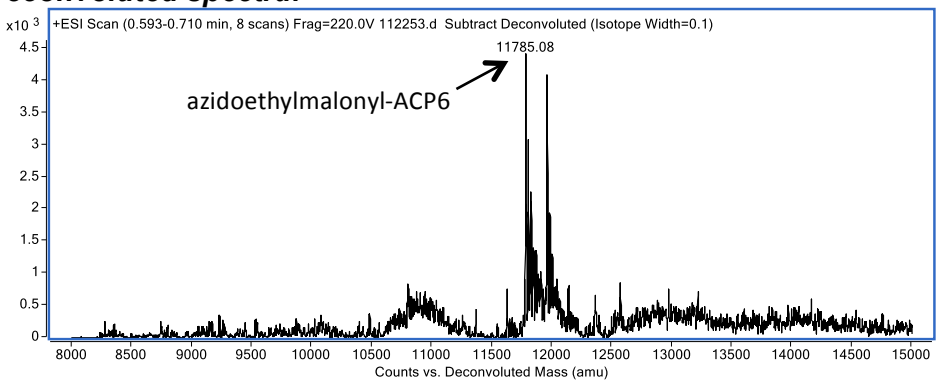

Deconvoluted spectra, expanded on target peak:

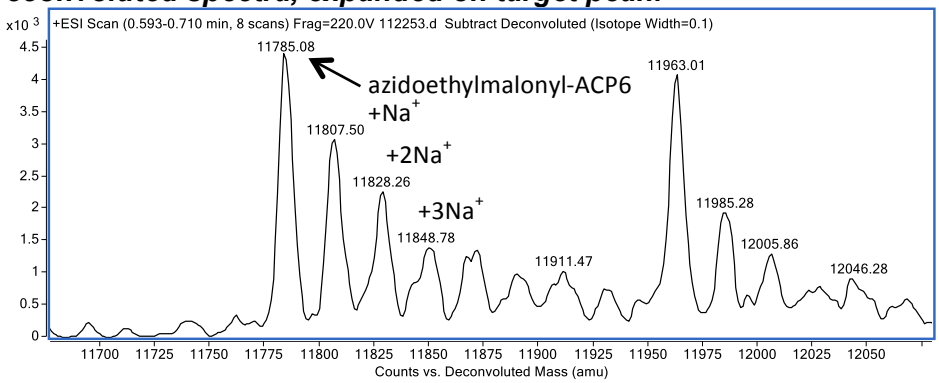

Component m/z:

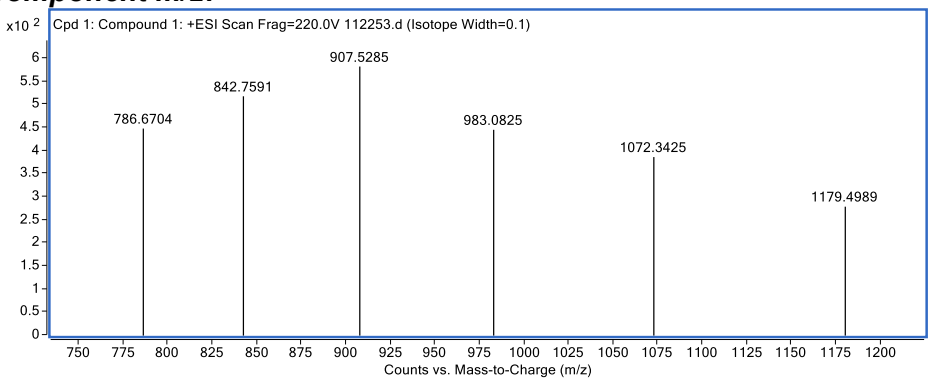

Component charge state:

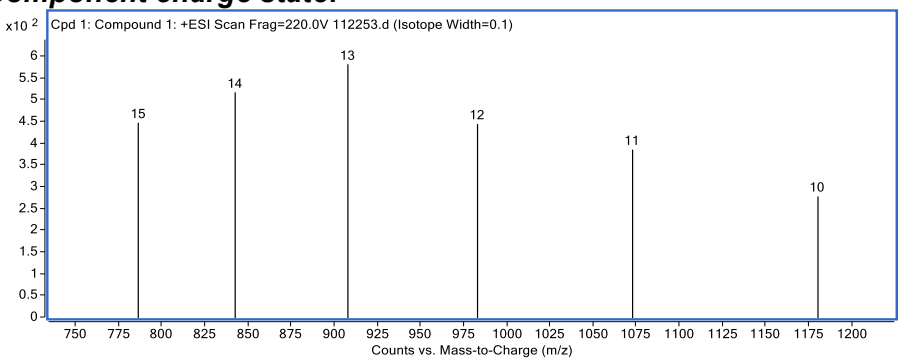

M) Negative control containing Sfp and DEBS *apo*-ACP6, in the absence of acyl-CoAs

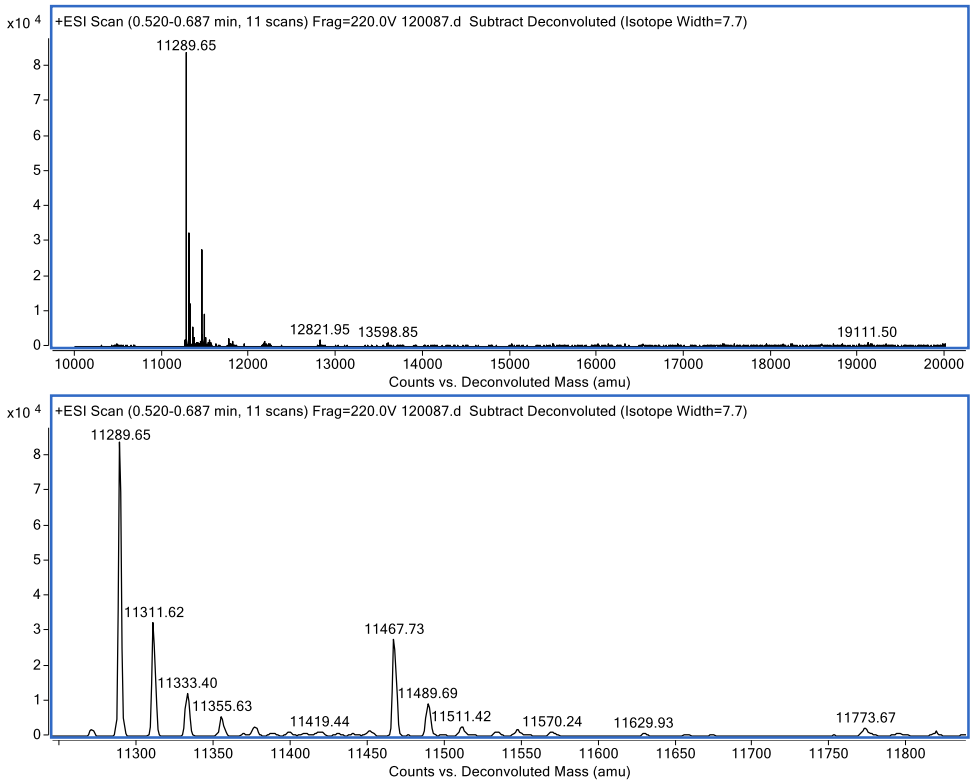

N) Negative control containing DEBS *apo*-ACP6 and 2a produced by WT-MatB, in the absence of Sfp

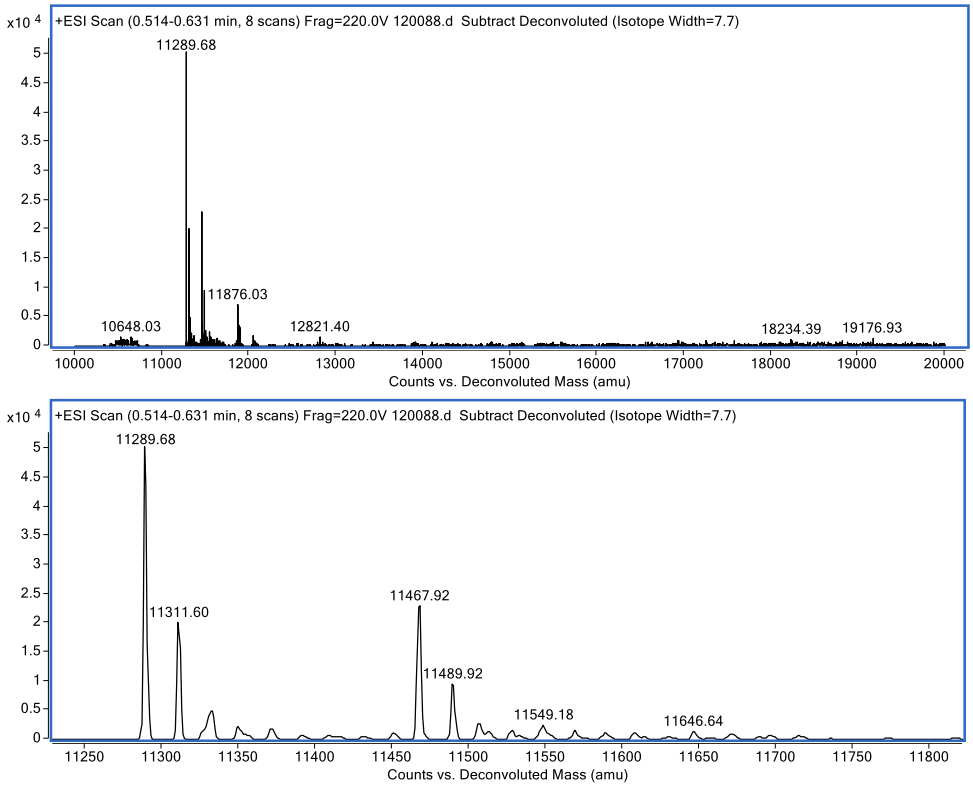

O) Negative control containing DEBS *apo*-ACP6 and 2b produced by WT-MatB, in the absence of Sfp

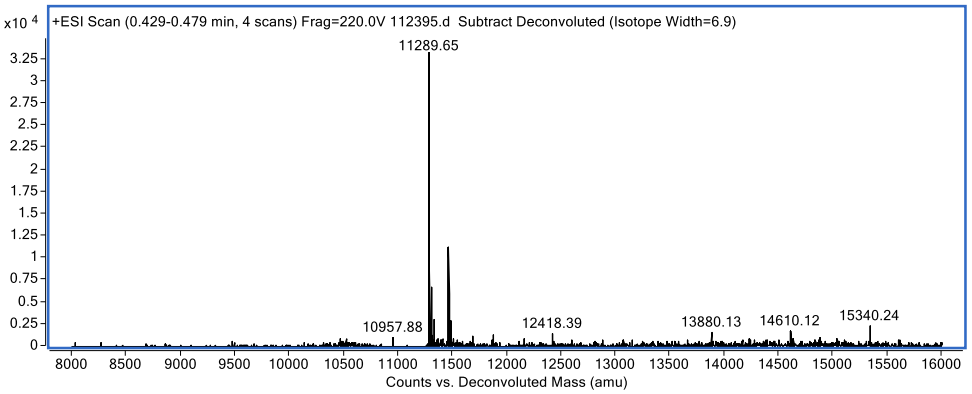

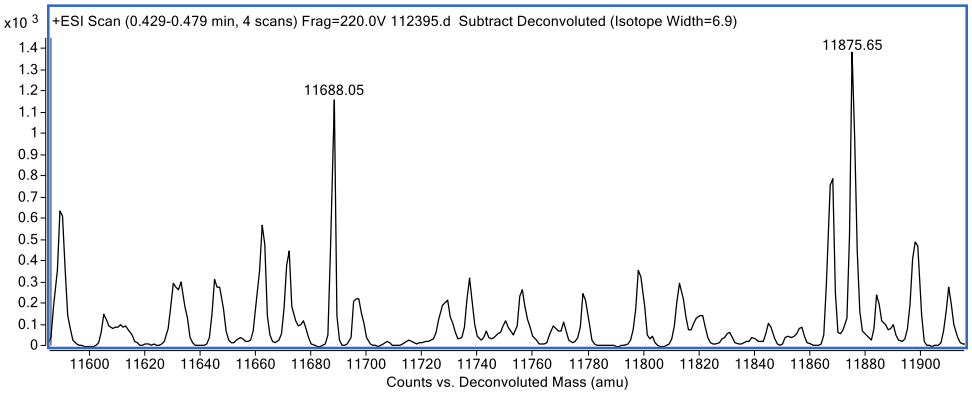

P) Negative control containing DEBS *apo*-ACP6 and 2c produced by MatB T207S/M306I, in the absence of Sfp

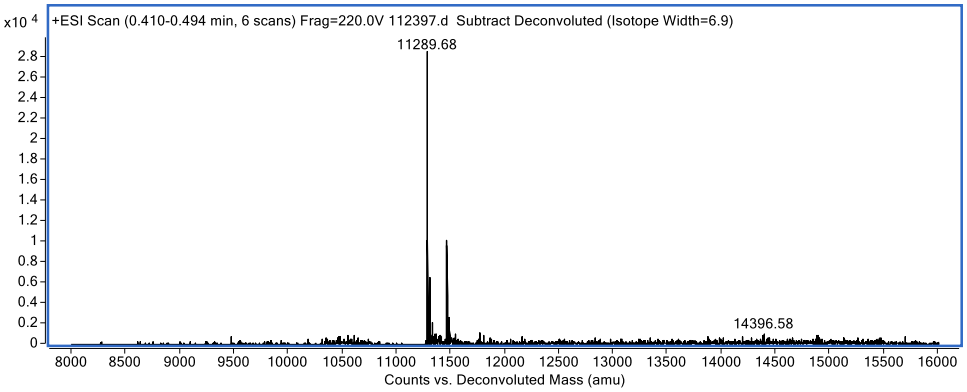

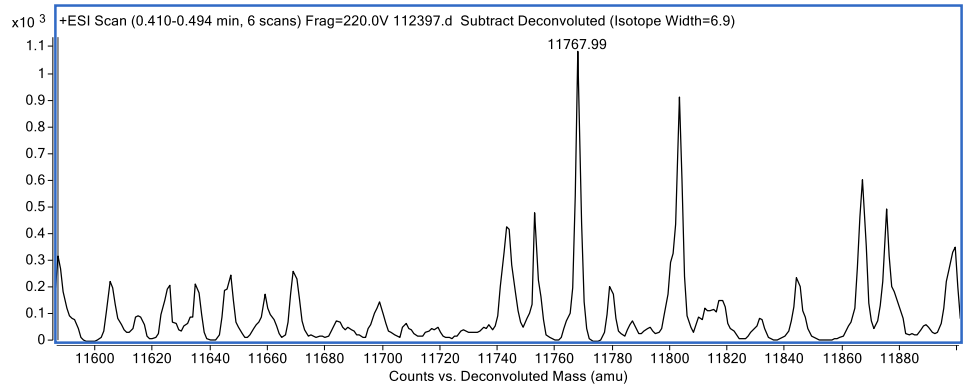

Q) Negative control containing DEBS *apo*-ACP6 and 2d produced by MatB T207G/M306I, in the absence of Sfp

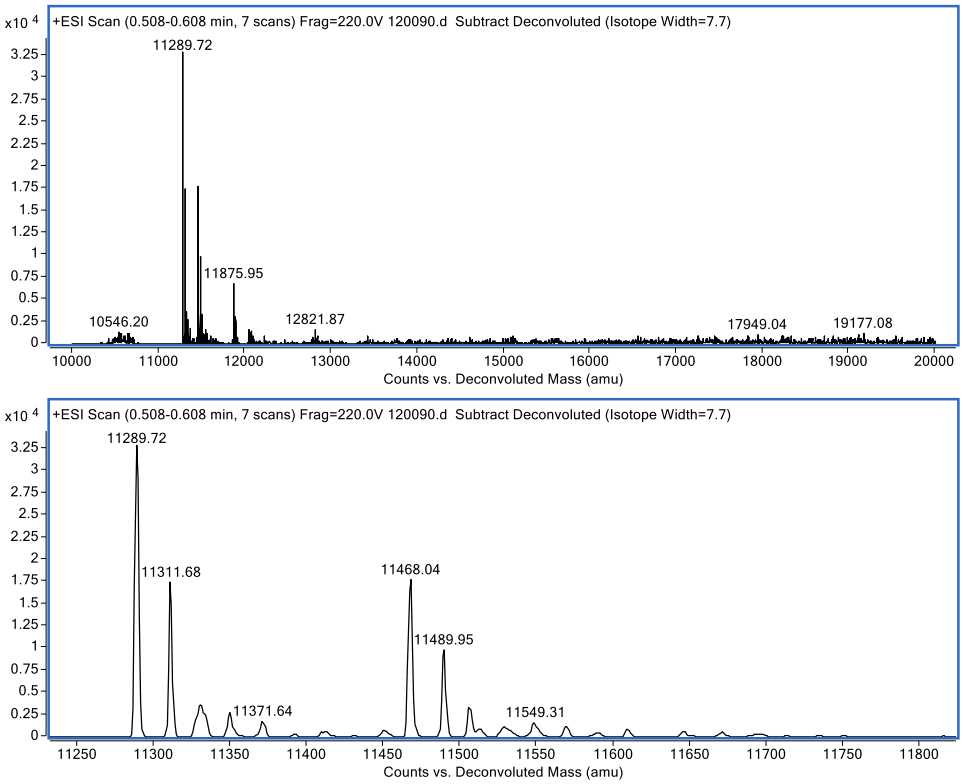

R) Negative control containing DEBS *apo*-ACP6 and 2e produced by MatB T207S/M306I, in the absence of Sfp

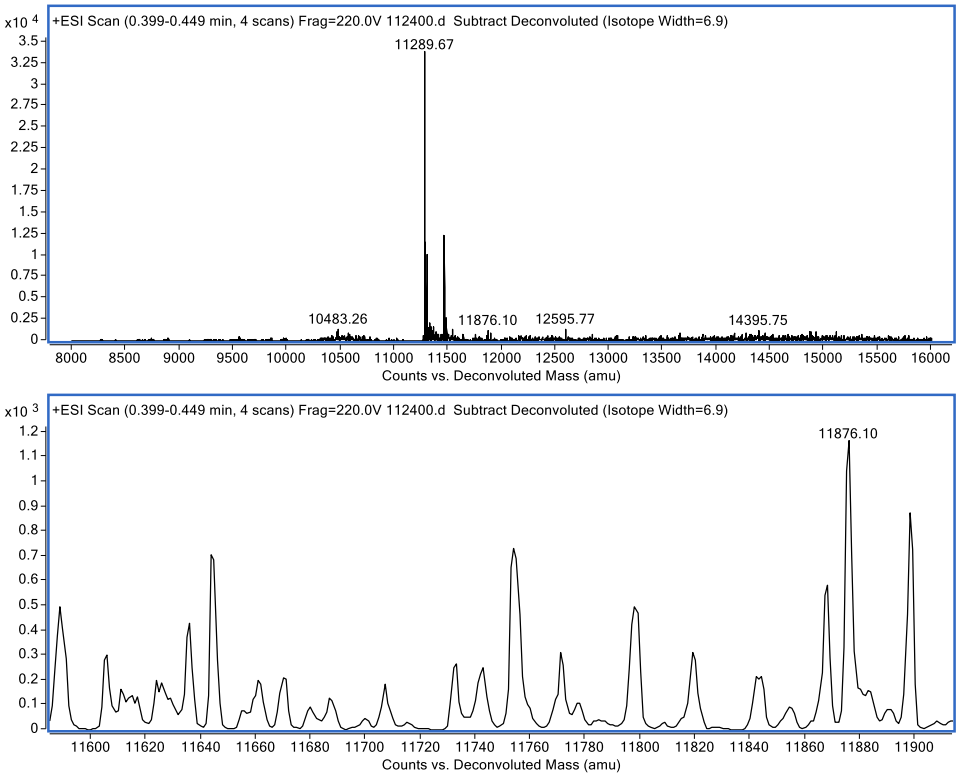

S) Negative control containing DEBS *apo*-ACP6 and 2f produced by MatB T207G/M306I, in the absence of Sfp

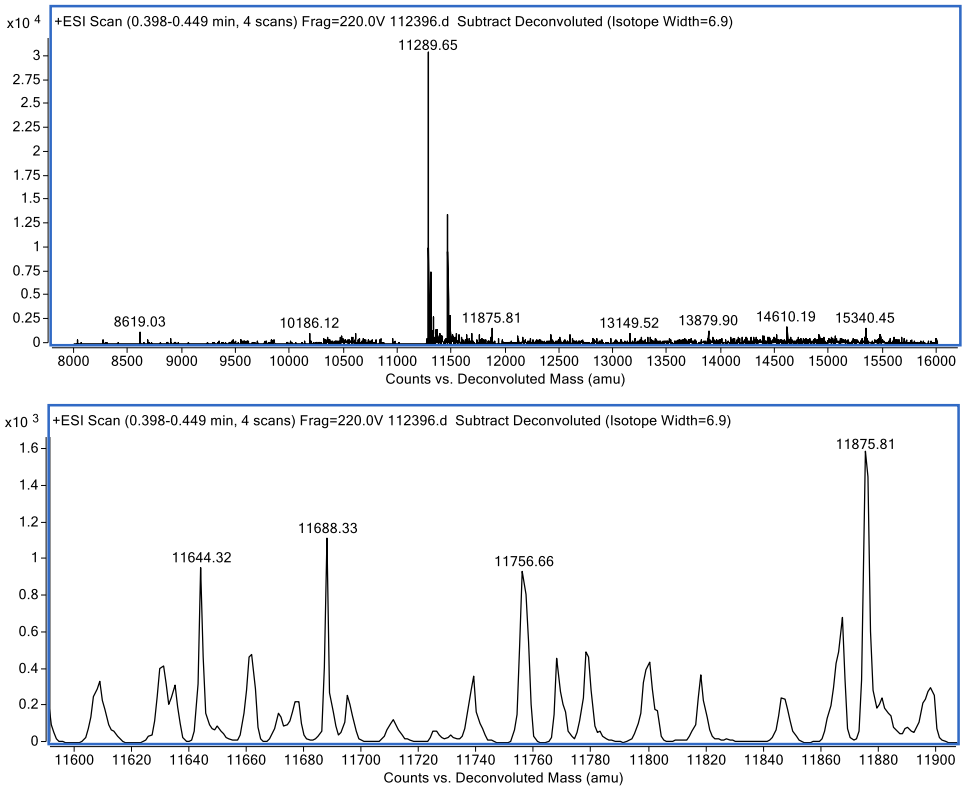

T) Negative control containing DEBS *apo*-ACP6 and 2g produced by MatB T207A, in the absence of Sfp

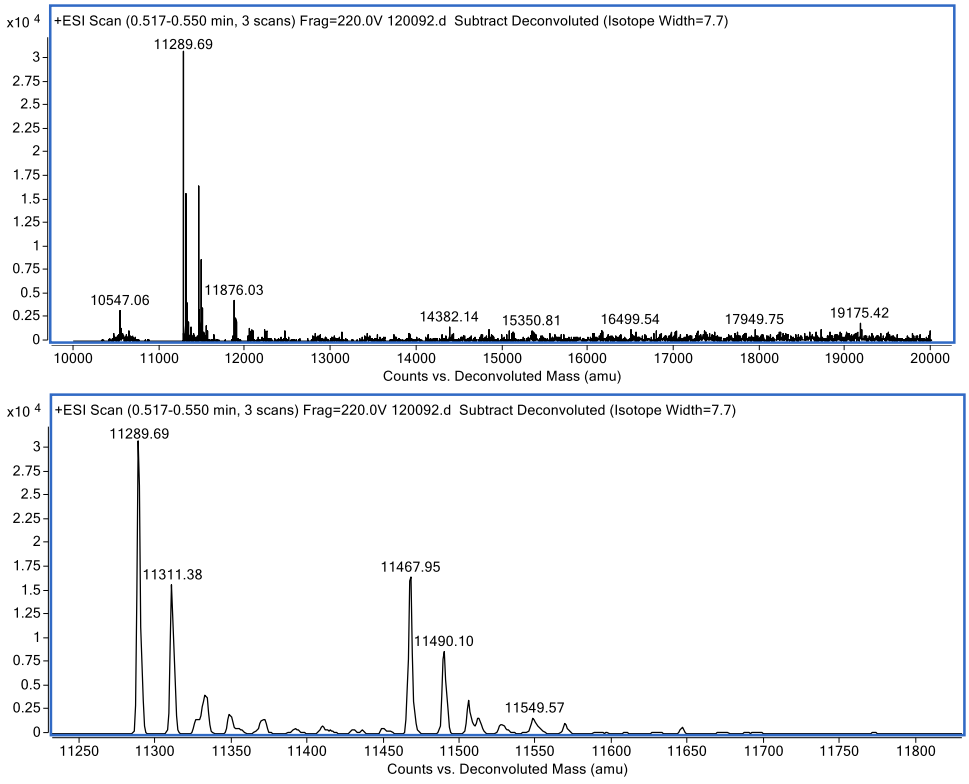

U) Negative control containing DEBS *apo*-ACP6 and 2h produced by MatB T207G/M306I, in the absence of Sfp

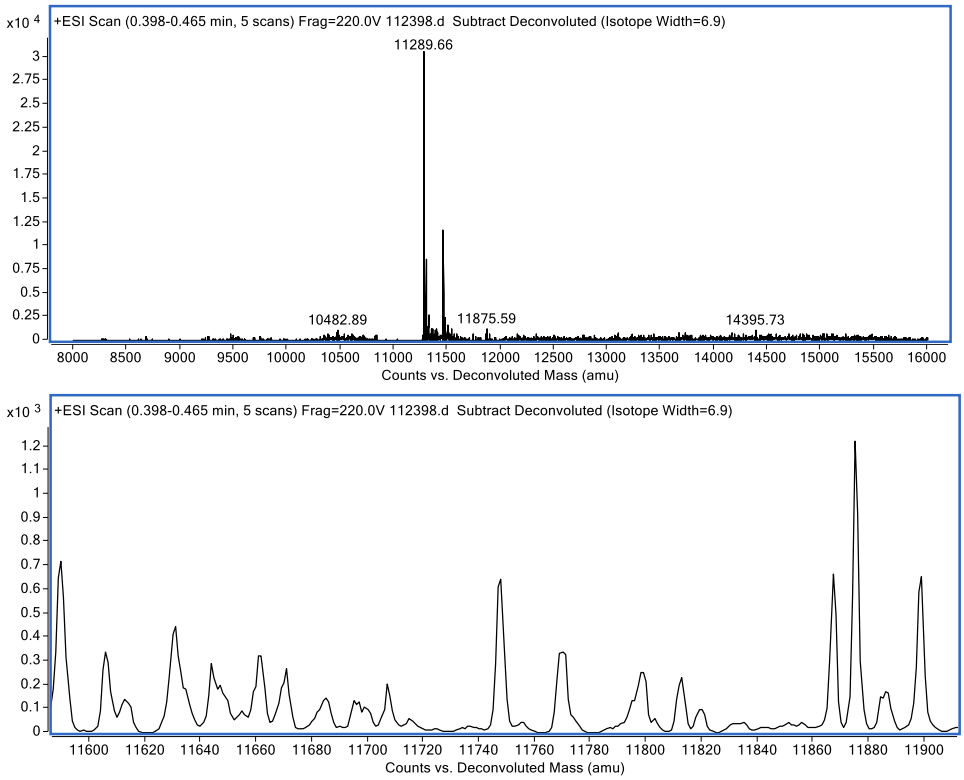

V) Negative control containing DEBS *apo*-ACP6 and 2i produced by MatB T207G/M306I, in the absence of Sfp

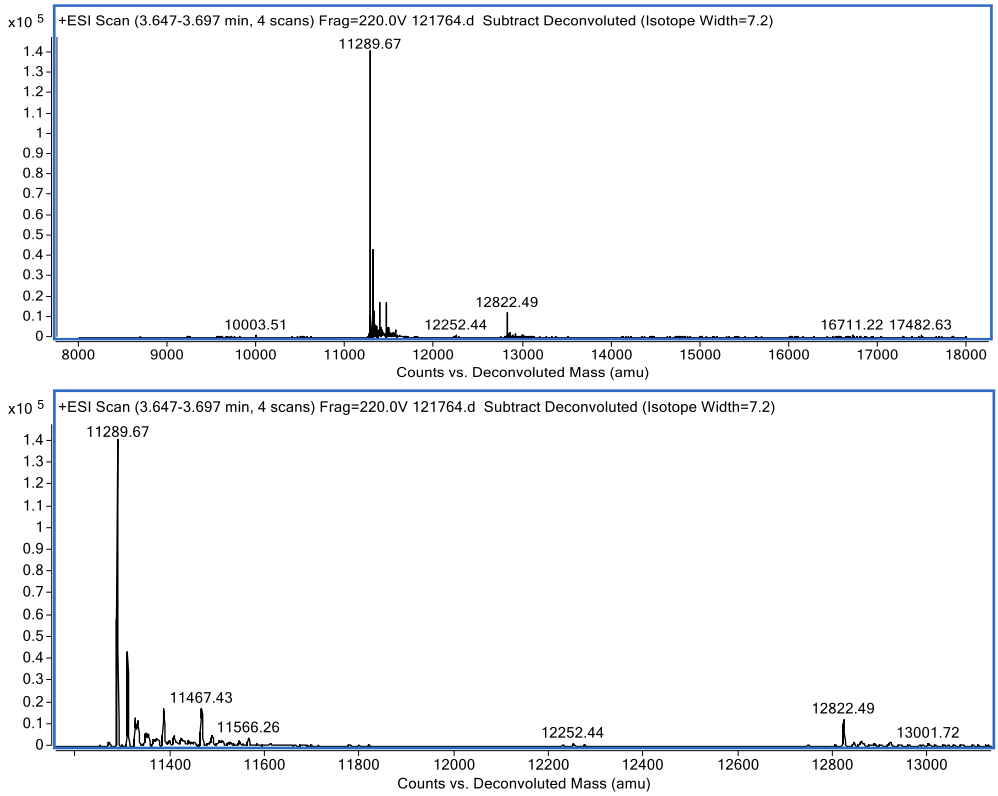

W) Negative control containing DEBS *apo*-ACP6 and 2j produced by WT MatB, in the absence of Sfp

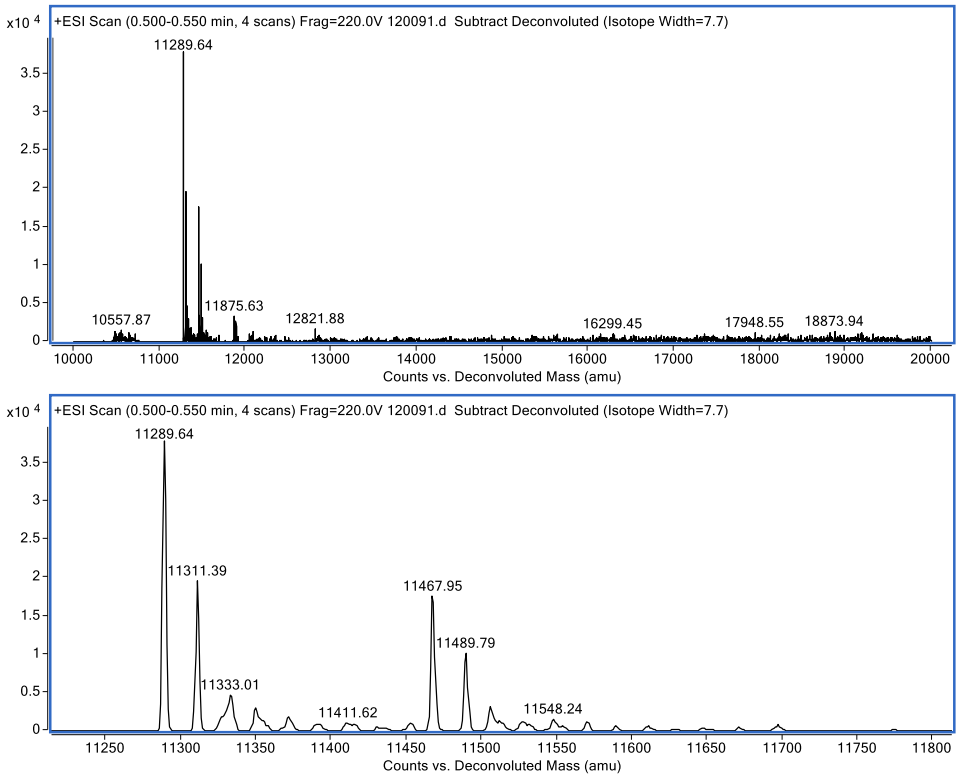

X) Negative control containing DEBS *apo*-ACP6 and 2k produced by MatB T207A/M306I, in the absence of Sfp

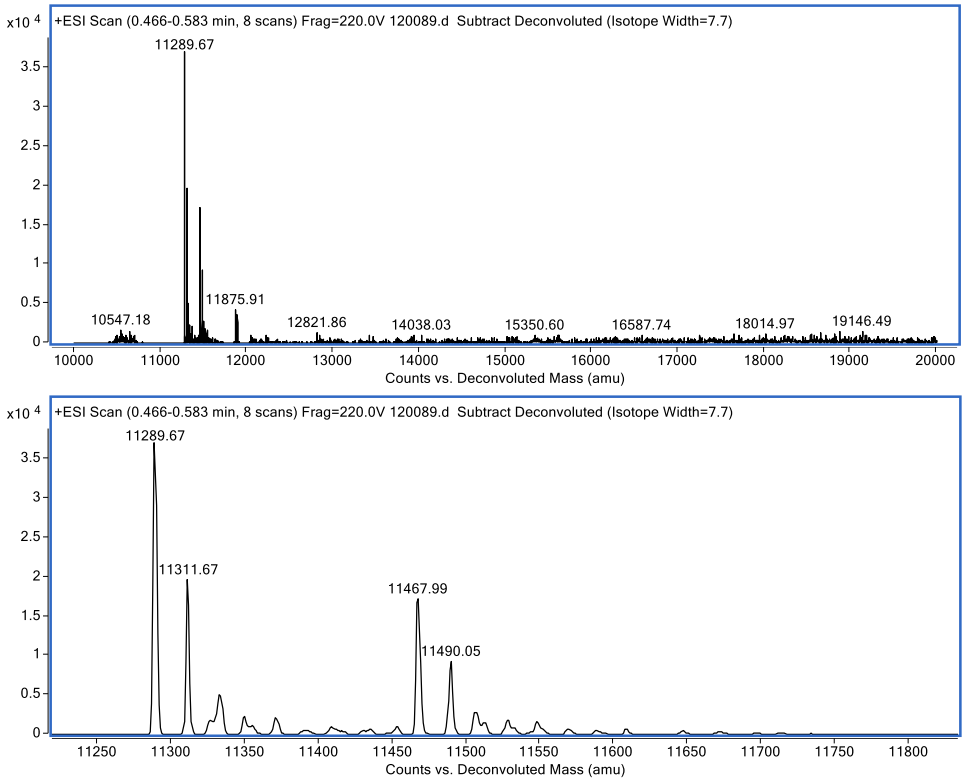

Y) Negative control containing DEBS *apo*-ACP6 and 2l produced by MatB T207G/M306V, in the absence of Sfp

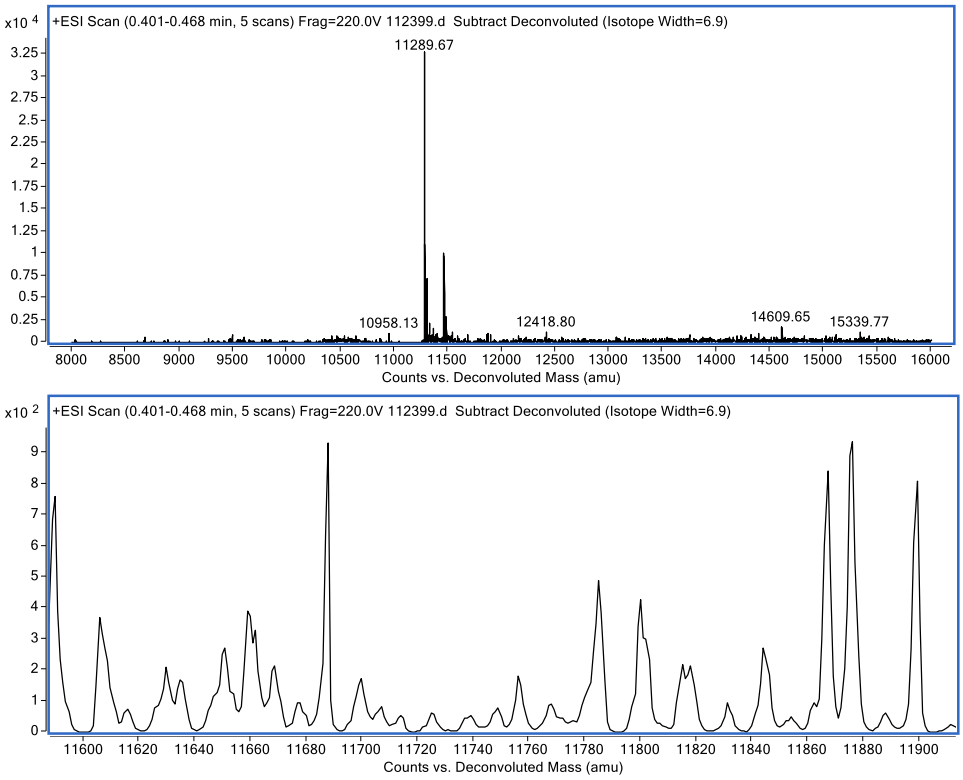

Table S3. ESI-MS analysis of Sfp-catalyzed acylation of DEBS *apo*-ACP6 using acyl-CoAs **2a**-**l**.

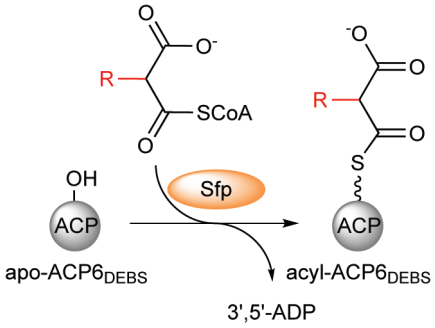

acyl-CoA[a]	acyl-ACP6$_{DEBS}$ calculated Mass (Da)[b]	acyl-ACP6$_{DEBS}$ observed mass (Da)[c]	predicted mass increase (Da)[d]	observed mass increase (Da)[e]
2a	11,715.99[f]	11,715.91[f]	426.01	426.18
2b	11,730.01[f]	11,730.13[f]	440.03	440.40
2c	11,744.02[f]	11744,16[f]	454.04	454.43
2d	11,754.01[f]	11,753.95[f]	464.03	464.22
2e	11,756.02[f]	11,756.02[f]	466.04	466.29
2f	11,758.04[f]	11,757.95[f]	468.06	468.22
2g	11,772.05[f]	11,772.10[f]	482.07	482.37
2h	11,748.01[g]	11,747.98[g]	458.03	458.25
2i	11,820.05[f]	11,820.09[f]	530.07	530.11
2j	11,731.99[f]	11,732.00[f]	442.01	442.27
2k	11,746.00[f]	11,746.03[f]	456.02	456.30
2l	11,785.02[f]	11,785.08[f]	495.04	495.35

[a] See Scheme 1 for structures of acyl-CoAs.

[b] Calculated (calc) mass for ACP6$_{DEBS}$ covalently modified with acylphosphopantetheine moiety of the corresponding acyl-CoA substrate. The calculated mass is adjusted to include loss of N-terminal methionine (-130.194 Da)

[c] Observed (obs) mass for ACP6$_{DEBS}$ covalently modified with acylphosphopantetheine moiety of the corresponding acyl-CoA substrate. Detected masses were not observed in control reactions that omitted sfp.

[d] $[\text{acyl-ACP6}_{DEBS}]_{calc} - [\text{apo-ACP6}_{DEBS}]_{calc}$

[e] $[\text{acyl-ACP6}_{DEBS}]_{obs} - [\text{apo-ACP6}_{DEBS}]_{obs}$

[f] $[M+H]^+$

[g] $[M-CO_2+H]^+$

Figure S9. Protein sequence used for exact mass determinations of *apo*-ACP6 from DEBS.

DEBS ACP6 (substrate for Sfp):

MGSSHHHHHHSSGLVPRGSHMAAPAREMTSQELLEFTHSHVAAILGHSSPDAVGQDQPF
TELGFDSLTAVGLRNQLQQATGLALPATLVFEHPTVRRLADHIGQQL

Figure S10. RP-HPLC analysis of the conversion of *apo*-AT^{o}-Mod6TE to triketide lactone using each extender unit and Sfp (i) **2a**, (ii) **2b**, (iii) **2c**, (iv) **2d**, (v) **2e**, (vi) **2f**, (vii) **2g**, (viii) **2h**, (ix) **2i**, (x) **2j**, (xi) **2k**, (xii) **2l**. Reactions included *apo*-AT^{o}-Mod6TE, Sfp, and diketide-SNAC **4**. Each sample was also analyzed by low res ESI-MS (Table S5). * indicates contaminants present in the **2g**-**2i** acyl-CoA preparations which were detected under the specialized conditions required for HPLC analysis of the resulting lactones. See Supplemental Information for assay conditions and detection methods.

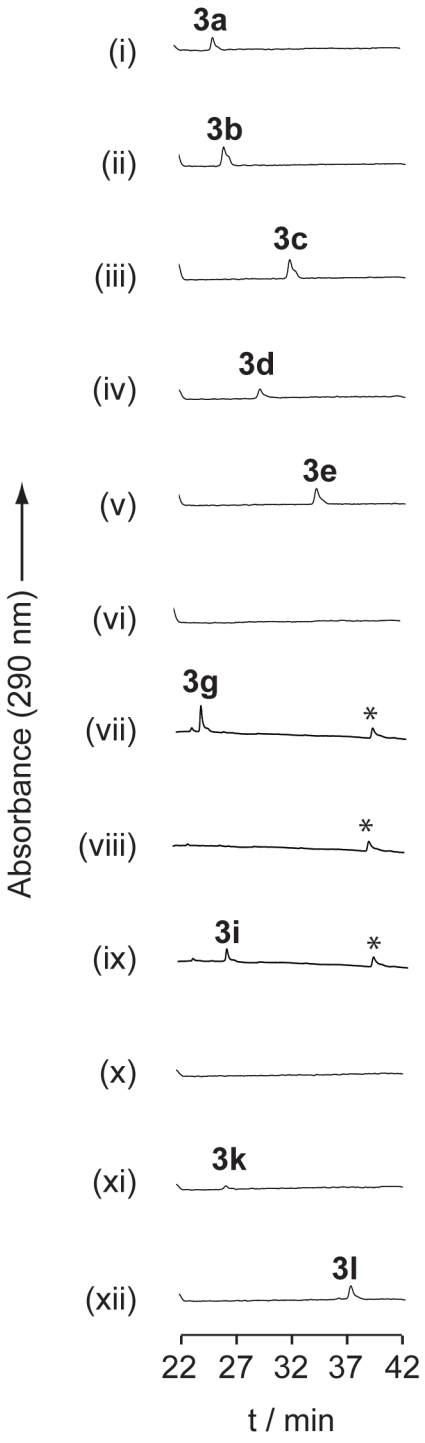

Table S4. LC-MS analysis of the conversion of *apo*-ATº-Mod6TE to triketide lactone using each extender unit and Sfp.

Acyl-CoA/ product[a]	Product retention time (mins)[b]	Relative conversion rate (%)[c]	Calculated mass[d]	Observed mass[e]
2a/3a	26.15	58	155.07	155.10
2b/3b	26.29	100	169.08	169.10
2c/3c	31.88	103	183.10	183.10
2d/3d	29.31	45	193.08	193.10
2e/3e	34.23	82	195.10	195.10
2f/3f	N.D[f]	N.D[f]	197.11	N.D[f]
2g/3g	23.72	58	211.13	211.10
2h/3h	N.D[f]	N.D[f]	231.10	231.10
2i/3i	25.96	33	259.13	259.13
2j/3j	N.D[f]	N.D[f]	171.06	N.D[f]
2k/3k	26.44	21	185.08	185.10
2l/3l	37.32	64	224.10	224.10

[a] See Scheme 1 for structures of acyl-CoAs and products. Acyl-CoA is transferred to *apo*-ATº-Mod6TE via Sfp (see Scheme 2)
[b] HPLC retention time. See Supplemental Information for HPLC conditions.
[c] Relative conversions were determined by HPLC and calculated by dividing the integrated area of the product from the non-natural acyl-CoA by the integrated area of the product from **2b**. Minimum detection limit is 1.6 % conversion. See Supplemental Information for reaction conditions.
[d] Calculated mass of triketide pyrone product, $[M+H]^+$.
[e] Observed mass of triketide pyrone product, $[M+H]^+$.
[f] N.D, non-detected. See Supplemental Information for LC-MS conditions.

Scheme S1